Polymer Testing 157 (2026) 109139

Contents lists available at ScienceDirect

Polymer Testing

journal homepage: www.elsevier.com/locate/polytest

Modified burn-off method for fiber content assessment in hemp and flax reinforced composites for marine structural applications

Jaewon Jang [a], Jean-Baptiste R.G. Souppez [b,*], Daekyun Oh [a,c,**]

[a] Center for Sustainable Ship Design, Industry-Academy Cooperation Foundation of Mokpo National Maritime University, Mokpo, 58628, Republic of Korea
[b] Department of Engineering, School of Architecture, Built Environment, Computing and Engineering, Birmingham City University, Birmingham, UK
[c] Department of Naval Architecture and Ocean Engineering, Mokpo National Maritime University, Mokpo, 58628, Republic of Korea

ARTICLE INFO

Keywords:
Fiber-reinforced polymer
Marine structures
Natural fiber-reinforced polymer
Burn-off method
Glass content
Internal defects

ABSTRACT

Fiber-reinforced polymers (FRPs), which are widely used in ship structures, have numerous advantages. However, environmental concerns exist regarding the raw materials' characteristics and challenges associated with disposal. Natural fibers such as hemp and flax are promising alternatives already applied in the automotive industry; nonetheless, their application to marine structures remains limited. Fiber content (*Gc*) measurements are crucial to satisfy structural design regulations, for which several methods exist. Among others, the burn-off method recommended by ISO 12215-5 and classification societies can accurately measure the *Gc* and internal defects of fiber composites. However, natural fibers have low ignition points, which renders the conventional burn-off method unsuitable. This study analyzed existing measurement techniques designed to assess *Gc* and internal defects considering the unique characteristics of cellulose-based natural FRPs (NFRPs). A modified burn-off method for NFRPs, which incorporates a pre-heating stage and adjusted combustion temperatures, is proposed to address the high moisture absorption and ignition point that are lower than those of resins inherent to natural fibers, overcoming the limitations of standard burn-off procedures. Experimental hemp and flax fiber composites were fabricated and their *Gc* was measured using various conventional methods and two proposed techniques: pre-heating followed by hydrometer testing and the modified burn-off method. Accordingly, the hemp specimens exhibited an average moisture absorption of approximately 2.623 ± 0.976 wt%, whereas that of the flax specimens was approximately 1.877 ± 1.115 wt%, and both were found to contain higher levels of internal defects compared to conventional glass-fiber-reinforced polymers. Overall, the modified burn-off method enables accurate quantitative evaluation of both *Gc* and internal defects in NFRPs.

1. Introduction

Fiber-reinforced polymers (FRPs) have high specific strength, excellent corrosion resistance, superior workability, and cost-effectiveness [1–5]. Consequently, they are widely used across various industries and their market demand is growing steadily [6–8]. In the marine sector, FRPs are commonly employed as structural hull materials for small vessels such as fishing boats, leisure crafts, and patrol boats, as well as superyacht structures recently [9–11]. However, the manufacturing and disposal of FRP vessels has drawn increased scrutiny in recent years, as global concern over environmental pollution continues to grow [12,13].

Marine-grade FRPs typically comprise a polymer matrix such as polyester or epoxy, combined with reinforcing fibers such as glass or carbon. These polymer matrices are derived from primary resources, including crude oil, natural gas, chlorine, and nitrogen, which presents clear environmental challenges [14]. Additionally, curing of these materials releases significant amounts of volatile organic compounds (VOCs), which not only pollute the air [15] but also pose health risks to workers during fabrication [16–18]. Glass and carbon fibers, the most common reinforcement materials, are synthetic and require energy-intensive production processes that emit toxic substances [19–21]. The automotive industry is subject to regulations that mandate the recycling of more than 85% of end-of-life vehicles [22]; however, the

* Corresponding author.
** Corresponding author. Center for Sustainable Ship Design, Industry-Academy Cooperation Foundation of Mokpo National Maritime University, Mokpo, 58628, Republic of Korea.
E-mail addresses: jb.souppez@bcu.ac.uk (J.-B.R.G. Souppez), dkoh@mmu.ac.kr (D. Oh).

https://doi.org/10.1016/j.polymertesting.2026.109139
Received 12 November 2025; Received in revised form 26 January 2026; Accepted 5 March 2026
Available online 6 March 2026

marine sector lacks similarly robust standards. Existing frameworks, such as the Hong Kong International Convention of the International Maritime Organization (IMO) [23] and the European Union's Ship Recycling Regulation [24], address dismantling procedures but do not provide specific targets or guidelines for FRP vessel disposal [25]. Although FRP recycling methods have been developed, including mechanical processing, pyrolysis, thermal decomposition, solvolysis, and chemical treatment [26,27], these approaches are often costly [28]. Furthermore, recycled fibers tend to be shorter and exhibit weak bonding with resins, yielding lower mechanical performance [26,29]. Consequently, incineration and landfilling remain the most common disposal methods, and FRP vessels are frequently abandoned along coastlines [30]. These practices can cause serious environmental damage, including dioxin and VOC release during incineration [31], along with microplastic pollution from weathered FRP debris [32].

Accordingly, alternative hull-construction materials are being explored [33,34]. These can be broadly categorized as carbon-intensive or low-carbon, based on the environmental impact of their production. Among carbon-intensive materials, aluminum and high-density polyethylene (HDPE) are of particular interest. Both exhibit high specific strength and good corrosion resistance, and both are recyclable. However, aluminum is costly and forming limitations arise regarding its application to complex hull geometries [35], whereas HDPE is hindered by manufacturing complexity, structural performance, and thermal resistance limitations. Although both are recyclable, their production is energy-intensive and heavily dependent on fossil fuels. Natural-fiber-reinforced polymers (NFRPs) have emerged as a low-carbon alternative. These composites typically comprise either animal- or plant-based fibers. The animal fibers employed in NFRPs include silk, wool, and spider silk, all of which comprise proteins [36]. Plant fiber sources include bast, leaves, or seeds, which are subjected to fiber extraction processes [37,38]. In industrial applications, plant-based fibers are more widely used because of their availability, cost efficiency, and ease of processing. Hemp and flax are especially common [36,39,40]. These materials are considered as carbon-reducing because plants absorb CO_2 during growth. Additionally, hemp and flax are relatively inexpensive compared to glass fibers [41,42], and their lower density [43,44] and high biodegradability at end-of-life render them attractive environmentally friendly alternatives [41,45]. However, hemp and flax fibers comprise cellulose, hemicellulose, lignin, and pectin [46], and typically contain 10%–12% moisture [47,48], which becomes a source of internal defects during composite fabrication. To reduce moisture absorption, various surface treatments have been developed, including alkaline, silane, acetylation, heat treatment, coating, and plasma processes [49–55]. These treatments modify the fiber prior to composite fabrication. However, research on accurate fiber content (*Gc*) determination for completed NFRPs, especially methods that reflect the absorbed moisture, remains limited.

FRP hull structural designs share many similarities with conventional ship designs; however, the former include a distinct stage for material specification. FRP hulls are designed according to ISO 12215-5 [56] or classification society rules, as illustrated in Fig. 1 [57]. The hull laminate thickness is determined based on the main ship characteristics, including speed, displacement, stiffener spacing, compartment configuration, and design loads, as well as the composite's material properties [9,58]. The material design influences mechanical performance and involves various factors, including fiber type, reinforcement form, fiber weight fraction (glass content, *Gc*), manufacturing method, and quality control [59]. Among them, *Gc* and fabrication quality are especially crucial, as they directly affect structural strength and safety. Therefore, international standards and classification society rules provide equations to estimate the mechanical properties of laminates based on *Gc*. These formulations are available for conventional synthetic fibers; however, no such models currently exist for natural fibers, as their use in marine applications is relatively new [11].

One of the most crucial quality factors impacting FRP laminate fabrication is the presence of internal defects. As a result of the inherent characteristics of composite processing, FRP laminates often exhibit porosity, voids, and delamination [60]. These defects are influenced by various parameters, including the fabrication environment (temperature and humidity), manufacturing method, operator proficiency, reinforcement type, and matrix properties [9]. The volume occupied by

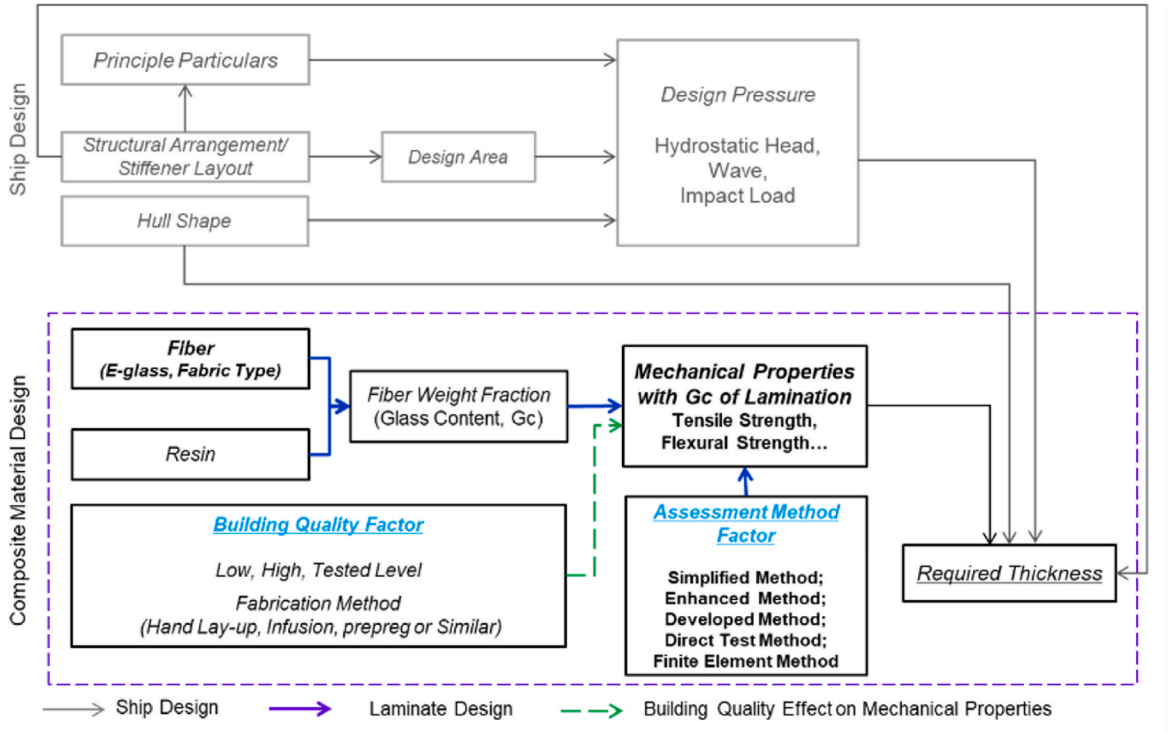

Fig. 1. FRP hull-laminate scantling flowchart from ISO 12215-5 [57].

voids is considered to have no effect on mechanical performance. Therefore, such regions are treated as having zero mechanical strength and density, while making no contribution to the stiffness or durability. Consequently, internal defects significantly degrade the mechanical properties of FRP laminates [61–63]. The laminate thickness required for marine applications generally exceeds that required in other sectors. In particular, naval vessels and other special-purpose ships often require laminate thicknesses of several tens of millimeters. Furthermore, composite shipbuilding requires a higher resin content than that necessary in other industries [64], which increases the propensity for void formation [65]. Natural fibers further amplify this challenge as they are hydrophilic and absorb considerable moisture, which increases the fiber weight and causes deviations in *Gc* measurements. This discrepancy can compromise the structural safety of the resultant vessel. Therefore, accurate *Gc* and internal defect assessment is essential to ensure the structural integrity of FRP laminates. This requirement applies equally to NFRPs made from hemp and flax.

To apply NFRPs in marine structures, it is essential to evaluate the *Gc* and internal defects accurately. Although various methods are available to assess these properties in FRP laminates, the burn-off test is known for its high accuracy [9]. However, this method was developed for synthetic fiber composite laminates with a specified burn-off temperature of approximately 600 °C, whereas hemp and flax fibers burn at approximately 200–300 °C, rendering the current burn-off method unsuitable [66–68]. At this temperature, not only the resin but also the natural fibers combust, resulting in the loss of the target reinforcement material. Another limitation is the inability of this approach to account for the moisture absorbed within the natural fibers, which makes accurate *Gc* determination difficult.

Accordingly, this paper proposes a modified burn-off method adjusted for the unique moisture-absorption and ignition characteristics of natural fibers for accurate *Gc* and internal defect measurement in NFRPs. Experimental specimens, which were fabricated using industrial-grade hemp and flax fibers, were evaluated using three standard methods for *Gc* measurement in FRP ship structures. The corresponding results were compared with measurements conducted using the modified burn-off method to analyze its reliability.

The remainder of this paper is organized as follows. Section 2 reviews existing *Gc* and internal defect measurement methods in FRP laminates and discusses its limitation for NFRP application. Section 3 analyzes the burn-off method according to ASTM D3171-15 [66] and defines the research method for NFRP applications. Section 4 analyzes the high moisture absorption and low ignition point of natural fibers and proposes a suitable modified burn-off method. Section 5 presents the specimen manufacturing and measuring processes using the standard methods for FRP ship structures and the modified burn-off method. The main results and implications are presented and discussed in Section 6. Finally, Section 7 summarizes the main contributions of this study, highlights the effectiveness of the modified burn-off method, and presents potential future research directions.

2. Standard methods for *Gc* and internal defect measurement in FRP ship structures

Precise *Gc* and internal defect measurement is essential to ensure the structural safety of FRP laminates in marine applications. The same requirement applies to NFRPs manufactured from hemp and flax, which are increasingly being considered as alternative hull materials. This section reviews the existing techniques used in the shipbuilding industry for *Gc* and internal defect assessment in FRP laminates. The primary techniques used to determine *Gc* in composite ship structures include rule-based calculations, direct measurement, hydrometer-based testing, and the burn-off method [58]. Table 1 summarizes the key characteristics of each method. The remainder of this section provides a detailed analysis of these approaches.

The rule calculation approach is commonly used for *Gc* estimation in FRP laminates. This method is based on the laminate thickness, which is determined via ISO 12215-5 or classification society rules, and involves back-calculation of G_c from the fiber and resin densities, along with the fiber weight per unit area, as follows:

$$G_c = \frac{\rho_r}{(\rho_r \rho_m)\, t/W + (\rho_r - \rho_m)}, \tag{1}$$

where ρ_f is the fiber density (g/cm^3), ρ_m is the resin density (g/cm^3), W is the fiber weight per unit area (kg/m^2), and t is the laminate thickness (mm). As destructive testing is not required, this method is simple and has been widely adopted in FRP ship design.

Direct measurement is an alternative *Gc* calculation approach, which involves measurement of the weight and dimensions of a laminate specimen. The relative density (ρ_c) is first determined from the cross-sectional area and thickness using Eq. (2); then, *Gc* is calculated from the fiber and resin densities using Eq. (3).

$$\rho_c = \frac{m_i}{100\, A\, t}, \tag{2}$$

$$G_c = \frac{0.1\, p\, N}{\rho_c\, t}, \tag{3}$$

where m_i is the laminate specimen weight (g), A is the cross-sectional area (m^2), t is the laminate thickness (mm), p is the weight of one ply or lamina of FRP per unit area (g/m^2), and N is the number of plies in the specimen.

Although this method is relatively straightforward, it is assumed that the laminate has a perfectly rectangular shape and that both the volume and weight can be measured precisely. In reality, laminate surfaces are often rough and irregular, and these characteristics can reduce the accuracy of this approach. For improved precision, a variant of the direct measurement method has been developed, in which a hydrometer is used for density measurement, following ASTM D792-13 [69]. Then, the resultant density value is used in Eq. (3) for more accurate *Gc* calculation. This approach is referred to as the hydrometer-assisted direct measurement method.

Table 1
Comparison between different *Gc* determination methods [58].

Glass Fiber Weight Fraction Measurement			
Rule Calculation	Simple Direct Measurement	Hydrometer-based Method	Burn-off Method
■ ISO 12215-5 reports the glass fiber and resin densities. *Gc* can be calculated based on these values and the structure thickness ■ This method is widely recommended by classification societies ■ The calculation is simple and the weight can be easily estimated from the laminate thickness ■ ISO 12215-5 and ASTM D792-13	■ The volume and weight are measured using tools such as a Vernier caliper and a scale; and the relative density is calculated ■ The procedure is very simple ■ The volume errors of some external shapes can be estimated ■ ASTM D792-13	■ The relative density of a cut laminate structure is measured using a tool such as a densimeter ■ A relatively accurate *Gc* value can be obtained using a simple tool ■ Interior defects such as voids cannot be considered ■ ASTM D792-13	■ The fiber weight within a laminate is measured by calcining a resin matrix using a furnace, and *Gc* is calculated based on the weight ■ *Gc* can be accurately calculated ■ A special experimental tool is required ■ The volume of the fabrication defects within the laminate can be considered ■ ASTM D3171-15, ISO 1172, and ASTM D792-13

The resin ignition test (hereafter referred to as the burn-off method) is another technique widely recommended for FRP applications, most notably in ISO 12215-5 and classification society guidelines. Unlike the previous three approaches, in this method, actual specimens are used to determine the fiber-to-resin ratio. In accordance with ASTM D3171-15 [66], the resin is either chemically dissolved or thermally removed to enable the measurement of the pure fiber weight and *Gc* calculation. The fibers used in FRP ship structures can be deformed by the acid solvent used for digestion; therefore, the burn-off method is more appropriate [58]. This method leverages the difference in combustion temperatures between the matrix and resin for the burn-off method according to ASTM D3171-15 [66] and ISO 1772 [70], 565 ± 30 and 625 °C, respectively. By contrast, conventional glass fibers begin to melt at a much higher temperature, approximately 1100 °C.

In addition to the fiber content, internal defect assessment in FRP laminates is crucial, as they directly influence structural integrity. Common techniques for internal defect detection include X-ray computed tomography (CT), ultrasonic testing, serial sectioning, and the burn-off test. CT imaging enables highly accurate visualization of internal voids but is limited by high costs and long processing times. Ultrasonic testing can identify internal defects; however, multiple samples are required to establish material-specific relationships between voids and signal attenuation. Serial sectioning yields excellent precision but incurs in significant time and labor costs. Furthermore, although these methods exhibit excellent performance in terms of defect location, they are less accurate when quantifying the total void volume [70–74]. By contrast, the burn-off test is a fast and practical method for quantitatively measuring internal voids in FRP laminates [9,75]. It also enables simultaneous *Gc* measurement, making it particularly useful for both material quality and structural reliability assessment.

Therefore, the burn-off test is widely regarded as the most suitable method for *Gc* and internal defect evaluation in FRP ship structures. However, this method exhibits significant limitations when applied to NFRPs comprised of natural fibers such as hemp and flax. This is due to the considerably low ignition point of conventional natural fibers where decomposition occurs at approximately 215 °C; therefore, they tend to combust before the resin during thermal treatment. Consequently, direct application of ASTM D3171-15-based burn-off methods to NFRPs is not possible.

To address this problem, a modified burn-off method tailored to the thermal characteristics of natural fibers is proposed in this paper. This revised method aims to enable accurate quantification of both *Gc* and internal defects in NFRP laminates.

3. Burn-off approach and research methods

Among the four standard methods for *Gc* determination in ship structures, the rule calculation, direct measurement, and hydrometer-based direct measurement methods can be applied to NFRPs. However, the burn-off method is not directly applicable because of the distinct thermal behavior of natural fibers. This section analyzes the conventional burn-off test procedure and presents a modified methodology suitable for NFRP applications.

3.1. Burn-off method according to ASTM D3171-15

ASTM D3171-15, titled "Standard Test Methods for Constituent Content of Composite Materials," provides procedures for quantitatively determining the constituents of composite materials, including the fiber, resin, and void volumes. This standard is divided into two main procedures: Test Methods I and II. Test Method I involves chemical or thermal removal of the resin to directly measure the fiber weight, enabling accurate *Gc* calculation. This method also enables void volume estimation using the relative composite density along with the fiber and matrix densities. Test Method II is a supplementary approach that enables *Gc* determination through non-destructive means based on dimensional and density measurements, similar to the direct measurement method discussed previously. Although simpler, this method is based on the assumption that no internal defects are present and, thus, tends to yield less accurate results. This study focused on a modified version of Test Method I, particularly the burn-off method, in which thermal decomposition is used for matrix removal. This choice was made over chemical digestion because of the fiber degradation risks and extended processing times associated with chemical methods [76].

The ASTM D3171-15 protocol specifies the required equipment and testing environment. An analytical balance with a resolution of at least 0.1 mg is necessary, and the muffle furnace must maintain a stable temperature of 600 ± 30 °*C*. For thickness measurements, the instrument should have a minimum resolution of 0.001 mm. The test must be conducted on a minimum of three specimens, each weighing at least 0.5 g. In cases where void volume evaluation is also required, the specimen weight must be at least 1.0 g. During specimen preparation, the dimensions must be measured with high precision. The weight should be recorded to the nearest 0.0001 g. The thickness should be measured at a minimum of 10 points, using a 4–7-mm micrometer interface for specimens with uneven surfaces, and the average should be used. The width and length should be measured at least three times each and their respective means calculated. The specimens must be placed in crucibles for combustion. Prior to testing, the crucibles must be cleaned by heating to 500–600 °*C* and cooled in a desiccator. The test should be conducted at 23 ± 5 °*C* with a relative humidity of less than 65%. Combustion is performed at 565 ± 30 °*C* until the weight stabilizes, for a maximum of 6 h, depending on the specimen size. A flowchart of this procedure is presented in Fig. 2.

Under the conditions described above, the specimen's *Gc* can be calculated by measuring its weight before and after combustion, following Eq. (4). Additionally, the specimen's internal defect volume can be determined using Eq. (5), based on the specimen density, initial and final weights after combustion, and fiber and resin densities.

$$G_c = 100\, M_f / M_i, \tag{4}$$

$$V_v = 100\, \left(1 - M_f \,/\, M_i\, \rho_c \,/\, \rho_f - \left(M_i - M_f\right) \,/\, M_i\, \rho_c \,/\, \rho_m\right), \tag{5}$$

where M_f is the final specimen weight after combustion (g), M_i is the initial specimen weight (g), ρ_c is the specimen's relative density (g/cm^3), ρ_f is the fiber density (g/cm^3), ρ_m is the resin density (g/cm^3), and V_v is the void volume (%).

3.2. Research method

Based on the analysis above, the standard burn-off method presents challenges when applied to NFRPs. Therefore, a reliable burn-off method for accurate *Gc* and internal defect measurement in NFRPs must incorporate the moisture retained within the natural fibers while also reflecting the lower ignition point of such fibers.

Accordingly, a pre-heating step is introduced to the proposed modified burn-off method to address the moisture absorption problem. Furthermore, the combustion temperature is adjusted to ensure that only the resin is removed, with no burning of the natural fibers; thus, their lower ignition threshold is accommodated. To validate the proposed modified burn-off method, a comparative analysis was conducted using five different methods: (i) rule calculation in accordance with international standards and classification society guidelines; (ii) direct measurement using the laminate's physical dimensions; (iii) hydrometer-based measurement using the relative density; (iv) hydrometer-based measurement after pre-heating to evaluate the effectiveness of the pre-heating process; and (v) the proposed modified burn-off method. For this comparative study, natural fibers that are widely used in industrial applications, namely, hemp and flax, were used to fabricate the NFRP specimens.

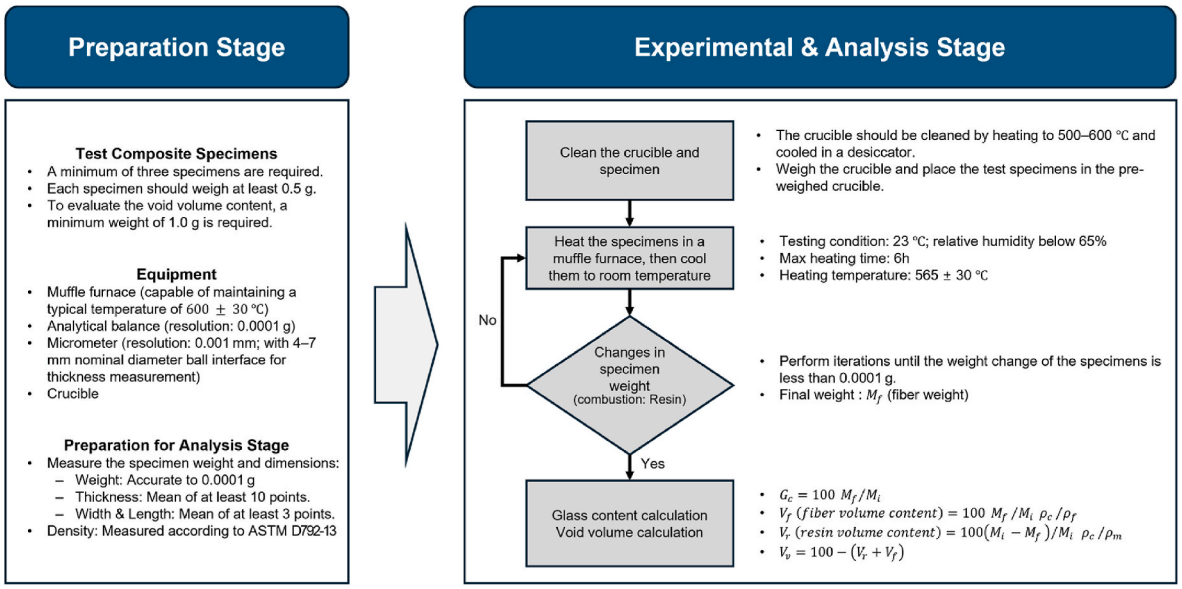

Fig. 2. Standard burn-off test procedure for FRP laminates according to ASTM D3171-15.

4. Modified burn-off method

This section builds on the ASTM D3171-15 test procedure discussed earlier and provides a detailed analysis of the high-moisture-absorption and low-ignition-point characteristics of natural fibers. Hence, a modified burn-off method suitable for NFRPs is proposed.

4.1. Moisture-absorption and low-ignition-point characteristics of natural fibers

Table 2 compares the characteristics of natural fibers and E-glass, a commonly used synthetic fiber in FRP applications. Among natural fibers, hemp and flax fiber composites have a lower flexural strength than glass fiber composites. However, their low specific gravity, which is approximately 40% lower than that of glass fiber composites, makes them attractive materials in various industries [78]. However, one of their limitations is their significantly higher moisture absorption compared to E-glass. This absorbed moisture can weaken the interfacial bonding or adhesion between the hydrophilic natural fibers and the polymer matrix, which is typically hydrophobic [36,79]. For glass-fiber-reinforced polymers (GFRPs) in composite form, moisture absorption is reported to be ~0.0093 wt% [80], whereas that of hemp and flax composites is significantly higher, ranging between 2.1 and 3.16 wt% [81,82]. Additionally, this absorbed moisture constitutes an internal defect, as it artificially increases the fiber weight and introduces errors in *Gc* calculations for laminates.

Another characteristic to consider is the low ignition point of natural fibers. As they have cellulose-based structures, natural fibers are inherently characterized by low thermal stability. The primary components of hemp and flax, namely, cellulose and lignin, begin to degrade at temperatures as low as 200 °C [67,68]. Although the decomposition temperatures vary with the exact fiber composition, most natural fibers begin degrading at approximately 215 °C [83]. For hemp and flax in composite form, degradation typically occurs at ~300 °*C* [84] and ~240 °*C* [85], respectively. These ignition points are significantly lower than that of E-glass, which does not begin melting until ~1000 °*C* [86]. Consequently, application of the conventional burn-off test to natural fiber composites causes simultaneous combustion of both the resin and fiber. By contrast, thermogravimetric analysis (TGA) results reported for commonly used diglycidyl ether of bisphenol A (DGEBA)-based epoxy resins indicate that the 5%-mass-loss temperature (T_{d5}) is approximately 330 °C [87]. This demonstrates a clear difference between the thermal degradation onset temperatures of hemp and flax fibers and that of the epoxy resin, indicating the existence of a temperature range in which the thermal behaviors of the two constituents do not interfere with each other's degradation characteristics. Therefore, to accurately apply the burn-off test to NFRPs, the procedure must consider both the moisture absorption and low ignition point of natural fibers. Only by addressing these two factors can the test reliably determine *Gc* and quantify the internal defects in the target laminate.

Table 2
Properties of natural fibers in relation to those of E-glass [77].

Property	Fiber		
	E-glass	Hemp	Flax
Density (g/cm^3)	2.55	1.48	1.40
Tensile strength (MPa)	2400	550–900	800–1500
E-modulus (GPa)	73	70	60–80
Elongation at failure (%)	3	1.6	1.2–1.6
Moisture absorption (%)	-	8	7

4.2. Modified burn-off method applicable to NFRPs

Based on the analysis presented in Section 4.1, in this study, the conventional burn-off method was modified to incorporate the high moisture absorption and low ignition point of natural fibers. The proposed modified burn-off method follows the procedure specified in ASTM D3171-15, with targeted adjustments to accommodate the specific properties of natural fibers. To address the issue of moisture absorption, a pre-heating step was introduced. Note that this step is essential for removing the moisture absorbed by the natural fibers and, thus, enabling accurate *Gc* measurement. The pre-heating temperature was determined based on TGA results for NFRP specimens, which revealed that moisture is released within a 25–155 °*C* range [88]. Additionally, the maximum temperature ensuring no moisture generation during natural fiber processing has been identified as 70 °*C* [89]. Therefore, the pre-heating process was defined as heating at 70 °*C* for 2 h.

The conventional burn-off test, which relies on the temperature difference between the combustion points of the fiber and resin to remove the resin at a lower calcination temperature, was modified by considering the low ignition point of natural fibers. Instead of resin

removal, the method was reversed such that the natural fiber is eliminated first, enabling measurement of the pure resin weight and, thus, more accurate *Gc* and internal defect determination. The experimental temperatures were selected based on the hemp- and flax-fiber degradation points reported in the literature. The temperature was set to 230 and 210 °*C* for hemp and flax, respectively. A flowchart of the modified burn-off test procedure tailored for NFRPs is presented in Fig. 3. The proposed method is compared with the conventional approach.

5. Application to hemp- and flax-fiber specimens

The preceding section discussed the development of a modified burn-off method to reflect the high moisture absorption and low ignition point of natural fibers. This section reports application of the proposed method to specimens fabricated using hemp and flax fibers. The specimens were produced via the hand lay-up and vacuum bagging methods, which are commonly used in the fabrication of ship structures. *Gc* was measured using the three standard methods that are widely applied to FRP ship structures, namely, rule calculation, direct measurement, and hydrometer-based direct measurement. This was done along with a method in which a pre-heating step was conducted prior to direct measurement and, finally, the proposed modified burn-off test. For NFRP fabrication, mat-type hemp and flax fibers with surface densities of 150 and 300 g/m^2, respectively, were used. Epoxy resin was used as the matrix material [90–92]. The relative density of the raw materials used for laminate fabrication was obtained from the manufacturers' technical datasheets. The density of both the hemp and flax fibers was set to 1.45 g/cm^3, while that of the epoxy resin was taken as 1.10 g/cm^3 [90–92]. The specimens were designed according to ISO 12215-5 and their design *Gc* was confirmed using Eq. (6) [56]. The specimens used for the experiments were cut to 40 × 40 mm using a waterjet cutting process (see Fig. 4). For each fiber type, six hand lay-up specimens and five vacuum bagged specimens were prepared, for a total of 22 specimens. The nomenclature for the specimens is in the following format: S_{fiber type, production method, specimen number}. The fiber type is "F" and "H" for the flax and hemp samples, respectively, while the production method is "H" and "V" for the hand lay-up and vacuum bagging methods, respectively. The design specifications for all specimens used in the experiments are summarized in Table 3.

$$G_{cDesign} = \rho_f \,/\, \rho_f \,\rho_m \,\left(T_{Design} \,/\, W_s + \left(\rho_f - \rho_m\right)\right), \tag{6}$$

where $G_{cDesign}$ is the designed fiber weight fraction (wt%), ρ_f is the fiber density (g/cm^3), ρ_m is the resin density (g/cm^3), T_{Design} is the designed specimen thickness, and W_s is the fiber weight in one ply of laminate (kg/m^2).

5.1. Method I – rule calculation

Using the material information for the fabricated specimens, the thickness per ply can be determined using Eq. (7) [56]. By multiplying this value by the number of plies in each specimen, the total laminate thickness can be calculated. This calculated thickness can then be applied to Eq. (1) to determine the specimen *Gc*. Once the design *Gc* is established, it can be used in conjunction with the thickness estimation formulas provided in the design rules to calculate the expected thickness. This approach also enables straightforward *Gc* back-calculation from the fabricated specimens.

$$T_{single\ ply} = W_s \,/\, \rho_f \,\rho_m \,\left(\rho_f \,/\, G_c - \left(\rho_f - \rho_m\right)\right), \tag{7}$$

where W_s is the fiber weight in one ply of laminate (kg/m^2), ρ_f is the fiber density (g/cm^3), ρ_m is the resin density (g/cm^3), and G_c is the fiber weight fraction (wt%).

5.2. Method II – direct measurement

The second *Gc* measurement method involves direct measurement of the shapes and weights of the laminate specimens. As shown in Fig. 5, measurements were conducted according to ASTM D3171-15. The length and width were each measured at three points in each sample, and the thickness was measured at thirteen points; hence, the average dimensions were determined for analysis. Because the specimen surfaces were uneven, a micrometer with a 6-mm tip diameter was used for the thickness measurement, following ASTM D3171-15 guidelines. In this study, thickness measurements were performed using a micrometer with a 0.001-mm resolution and a measurement uncertainty of ± 0.002 mm. The weight was measured to the nearest 0.001 g, which was the limit of the available equipment. To evaluate *Gc* uncertainty arising from the mass measurement resolution, an analysis was conducted under extreme-case assumptions. For specimen S_{F, H, 5}, which exhibited a relatively low fiber content, the mass measurement error was assumed to be ± 0.001 g, and *Gc* was recalculated accordingly. The resulting *Gc*

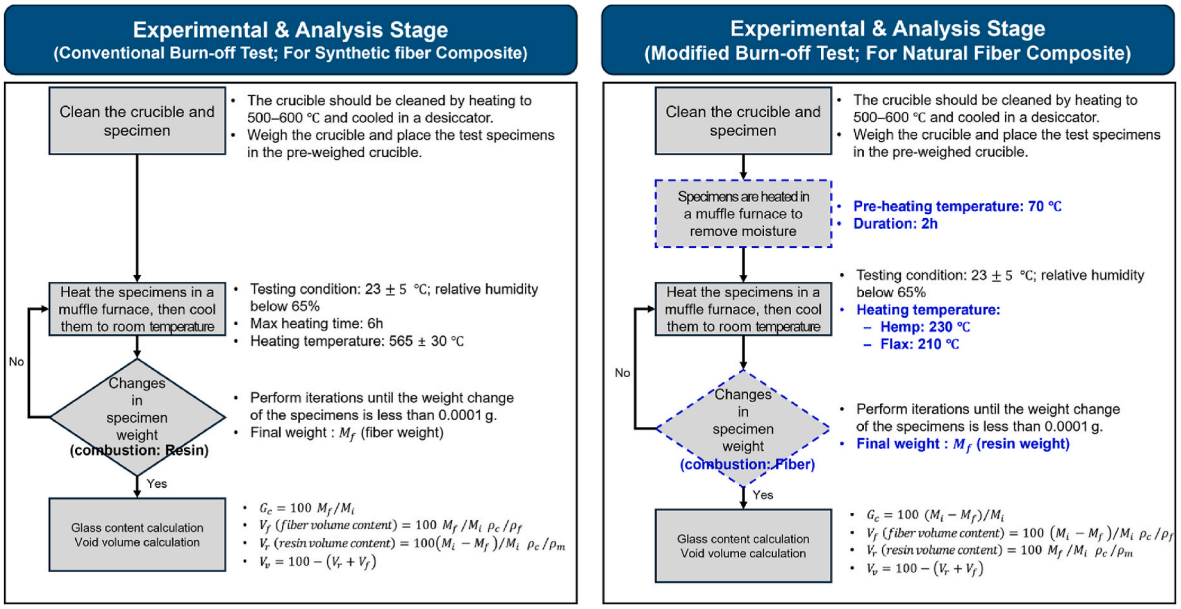

Fig. 3. Comparison between the conventional burn-off test and the modified burn-off test accommodating the properties of natural fibers.

(a) Hemp and flax fibers (b) Hemp fiber specimens by fabrication method (c) Flax fiber specimens by fabrication method

Fig. 4. Fibers and fabricated NFRP specimens used in this study.

Table 3
Design details of the NFRP specimens.

Fiber	Method	Design *Gc* (wt%)	Number of plies	T_{single} (mm)[a]	T_{design} (mm)[b]
Hemp	Hand lay-up	39.524	Mat × 9	0.312	2.809
	Vacuum bagging	37.746	Mat × 7	0.328	2.298
Flax	Hand lay-up	16.134	Mat × 4	1.625	6.498
	Vacuum bagging	21.617	Mat × 5	1.196	5.979

[a] T_{single}: specimen thickness per ply.
[b] T_{design}: designed specimen thickness.

values ranged between 16.834 and 16.843 wt%, corresponding to a difference of approximately 0.0030%. This variation is negligible compared with the differences in *Gc* observed among the specimens in this study, indicating that the influence of mass measurement uncertainty on the *Gc* results is limited and not statistically significant. The dimensions and weights measured from the hemp and flax specimens are reported in Tables 4 and 5, respectively. Although the specimens were cut precisely using a waterjet, some degree of dimensional error was observed. Additionally, thickness variability was evaluated by calculating the average coefficient of variation (CV) for the hemp and flax specimens according to the fabrication method. For the hemp specimens, the average thickness was approximately 2.819 and 2.269 mm for the hand lay-up and vacuum bagging methods, respectively; the corresponding CVs were 2.102% and 2.384%, respectively. For the flax specimens, the average thickness was approximately 6.503 and 5.981 mm for the hand lay-up and vacuum-bagged specimens, respectively; the corresponding CVs were 4.277% and 4.245%, respectively.

Based on the measured dimensions and weights, the calculated *Gc* values for the hemp and flax specimens are reported in Tables 6 and 7, respectively. For all specimens, discrepancies were observed between the *Gc* values obtained via Methods I and II. These differences can be attributed to variations introduced during laminate fabrication, particularly differences between the actual and designed specimen volumes. Comparing the thicknesses listed in Table 3 with the measured values reported in Tables 4 and 5, deviations between the calculated and actual thicknesses are apparent. This outcome reflects a general characteristic of FRP materials, where differences between the design values (Method I) and the actual fabricated results often arise. These findings confirm the importance of accurate *Gc* measurement in practice.

5.3. Method III –hydrometer-based direct measurement

The third method considered in this study was a refined version of

Table 4
Dimensional and weight measurements of the hemp specimens.

Specimen	Mean			Weight (g)
	Length (mm)	Width (mm)	Thickness (mm)	
S_{H, H, 1}	40.390	40.260	2.859	4.685
S_{H, H, 2}	40.560	40.337	2.741	4.513
S_{H, H, 3}	40.347	40.530	2.863	4.716
S_{H, H, 4}	40.497	40.233	2.888	4.734
S_{H, H, 5}	40.420	40.167	2.793	4.619
S_{H, H, 6}	40.183	40.420	2.769	4.559
S_{H, V, 1}	39.027	39.140	2.146	3.665
S_{H, V, 2}	39.073	38.930	2.376	3.870
S_{H, V, 3}	38.640	39.157	2.279	3.778
S_{H, V, 4}	39.097	38.790	2.291	3.780
S_{H, V, 5}	38.613	39.087	2.251	3.758

(a) (b)

Fig. 5. (a) Length and width of the specimens. (b) Thickness measurement locations for the hemp and flax specimens.

Table 5
Dimensional and weight measurements of the flax specimens.

Specimen	Mean			Weight (g)
	Length (mm)	Width (mm)	Thickness (mm)	
S_{F, H, 1}	39.927	40.097	6.633	11.011
S_{F, H, 2}	39.860	40.210	6.088	9.953
S_{F, H, 3}	40.090	39.893	6.485	10.255
S_{F, H, 4}	39.960	39.867	6.649	10.562
S_{F, H, 5}	40.043	39.867	6.868	11.373
S_{F, H, 6}	40.153	39.883	6.296	10.354
S_{F, V, 1}	40.257	40.353	6.168	9.052
S_{F, V, 2}	40.200	40.310	5.821	8.251
S_{F, V, 3}	40.283	40.233	5.927	8.026
S_{F, V, 4}	40.150	40.343	6.018	8.020
S_{F, V, 5}	40.250	40.407	5.973	8.256

Table 6
Gc results for the hemp specimens obtained via direct measurement.

Specimen	*Gc* (wt%) (Method II)
S_{H, H, 1}	46.857
S_{H, H, 2}	48.940
S_{H, H, 3}	46.811
S_{H, H, 4}	46.463
S_{H, H, 5}	47.451
S_{H, H, 6}	48.096
S_{H, V, 1}	43.762
S_{H, V, 2}	41.271
S_{H, V, 3}	42.050
S_{H, V, 4}	42.127
S_{H, V, 5}	42.170

Table 7
Gc results for the flax specimens obtained via direct measurement.

Specimen	*Gc* (wt%) (Method II)
S_{F, H, 1}	17.447
S_{F, H, 2}	19.324
S_{F, H, 3}	18.715
S_{F, H, 4}	18.100
S_{F, H, 5}	16.844
S_{F, H, 6}	18.560
S_{F, V, 1}	26.919
S_{F, V, 2}	29.459
S_{F, V, 3}	30.290
S_{F, V, 4}	30.295
S_{F, V, 5}	29.549

the previously conducted direct measurements, which is designed to yield more accurate *Gc* values by employing a hydrometer. Measurements were conducted in accordance with ASTM D792-13 [69]. A water-immersion-type hydrometer was used, with a resolution of up to 0.01 g/cm^3. The measurement accuracy of the instrument was ± 0.01 g/cm^3. Fig. 6 shows sample relative density measurements for flax specimens conducted using this hydrometer. The relative densities obtained through this process were then used for the *Gc* calculation. The *Gc* measurement results for the hemp and flax specimens are reported in Tables 8 and 9, respectively.

Based on these results, although some differences were observed compared to those obtained via Methods I and II, a similar trend is evident. Overall, the *Gc* values were lower than those calculated using Method II. This discrepancy was attributed to volume measurement errors in the specimen dimensions.

5.4. Method IV – direct measurement with pre-heating

The fourth method employed in this study was designed to accommodate the high moisture-absorption characteristic of natural fibers by incorporating a pre-heating process prior to *Gc* measurement. Based on prior literature regarding the temperature range for moisture release from natural fibers, as well as manufacturer guidelines, pre-heating was conducted at 70 °*C* in 30-min intervals for a total of 2 h. Pre-heating was performed using a muffle furnace employed for the burn-off test [93], which has a chamber volume of 4.5 L. The furnace is capable of operating at temperatures of up to 1200 °*C*, with a temperature accuracy of ± 5 °*C* and temperature uniformity of ± 10 °*C*. In this study, the pre-heating procedure was conducted by setting the furnace to a set temperature of 70 °*C*. During pre-heating, operator error regarding temperature control caused damage to one hand lay-up specimen (S_{H, H, 3}) and one vacuum bagging specimen (S_{H, V, 1}), which were excluded from further analysis. All experiments were conducted under the environmental conditions recommended in ASTM D3171, namely, a temperature of 23 ± 5 °*C* and a relative humidity of ≤65%. To minimize the effect of moisture reabsorption in NFRPs, the specimens were cooled in a humidity-controlled desiccator for approximately 10–15 min prior to measurement. Fig. 7 shows the conditions of selected specimens before and after pre-heating. After this process, the weight changes were recorded and the relative densities were measured using a hydrometer. The final *Gc* values for all hemp and flax specimens are reported in Tables 10 and 11, respectively.

The pre-heating process slightly reduced the masses of all specimens;

Table 8
Gc results for the hemp specimens based on the dimensions and hydrometer-determined relative density.

Specimen	Relative density (g/cm^3)		*Gc* (wt%) (Method III)
	By dimension	By hydrometer	
S_{H, H, 1}	1.01	1.07	44.133
S_{H, H, 2}	1.01	1.07	46.036
S_{H, H, 3}	1.01	1.05	44.901
S_{H, H, 4}	1.01	1.06	44.099
S_{H, H, 5}	1.02	1.06	45.599
S_{H, H, 6}	1.01	1.06	45.997
S_{H, V, 1}	1.12	1.17	41.825
S_{H, V, 2}	1.07	1.15	38.434
S_{H, V, 3}	1.10	1.16	39.711
S_{H, V, 4}	1.09	1.15	39.845
S_{H, V, 5}	1.11	1.15	40.567

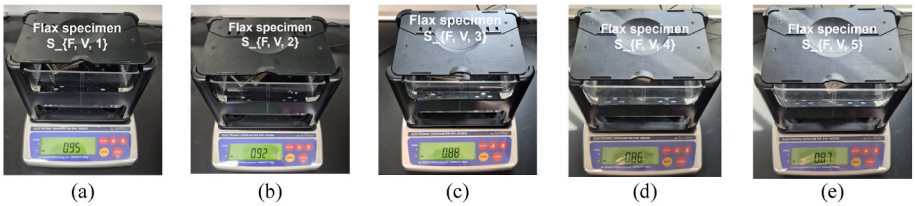

(a) (b) (c) (d) (e)

Fig. 6. Relative density measurements for the flax specimens conducted using a water immersion hydrometer: (a)–(e) Flax specimens S1–S5, respectively.

Table 9
Gc results for the flax specimens based on the dimensions and hydrometer-determined relative density.

Specimen	Relative density (g/cm^3)		*Gc* (wt%) (Method III)
	By dimension	By hydrometer	
S_{F, H, 1}	1.03	1.06	16.991
S_{F, H, 2}	1.02	1.06	18.596
S_{F, H, 3}	0.99	1.03	17.964
S_{F, H, 4}	1.00	1.03	17.522
S_{F, H, 5}	1.04	1.06	16.484
S_{F, H, 6}	1.03	1.07	17.812
S_{F, V, 1}	0.90	0.95	25.601
S_{F, V, 2}	0.87	0.92	28.010
S_{F, V, 3}	0.84	0.88	28.760
S_{F, V, 4}	0.82	0.86	28.982
S_{F, V, 5}	0.85	0.87	28.867

this was accompanied by a decrease in density. Therefore, the reduction was caused by the removal of the moisture absorbed in the fibers. As water was removed from within the fibers, the specimen masses decreased; however, the volume remained constant, which yielded a decrease in density. Consequently, the *Gc* values also decreased. For the hemp specimens, average moisture absorption values of 3.373 ± 0.536 (confidence interval (CI): 2.707–4.039) and 1.685 ± 0.218 (CI: 1.338–2.032) wt% were obtained for the hand-lay-up and vacuum-bagging specimens, respectively. For the flax specimens, the average moisture absorption values were 1.065 ± 0.178 (CI: 0.875–1.251) and 2.854 ± 0.938 (CI: 1.689–4.019) wt%, respectively. A comparison between the *Gc* results obtained with and without pre-heating (Tables 8 and 9) shows that laminates fabricated with hemp fibers exhibit an average impregnation ratio difference of 1.909 wt%, whereas those fabricated with flax fibers exhibit an average difference of 1.452 wt%. These values are consistent with those reported in previous studies [81, 82]. As can be seen in Fig. 7, there is convergence toward a stable value, suggesting that the pre-heating process was conducted under appropriate conditions. However, further research is needed to determine whether the observed weight changes due to moisture removal are statistically significant.

5.5. Method V – modified burn-off test

The final method applied in this study was the modified burn-off test, which was used to determine both the *Gc* and internal defects of the NFRP specimens. Based on the procedure described in Section 3, this method involved combusting the natural fiber using a muffle furnace and measuring the remaining resin weight for the *Gc* calculation and internal defect assessment. The test temperatures were selected considering the decomposition temperatures of the natural fibers and the NFRP degradation thresholds. Specifically, the test was conducted at 230 and 210 °*C* for the hemp and flax composites, respectively. The weight of each specimen was recorded at 20-min intervals and the test was repeated until the final weight change was within 0.001 g. Fig. 8 shows the experimental setup, including the muffle furnace and the desiccator used during the cooling phase. Each test was conducted under controlled environmental conditions, with the ambient temperature and relative humidity being maintained at 23 ± 5 °*C* and 65%, respectively.

Fig. 9 shows the weight change trends of the hemp and flax composites observed during the modified burn-off test. Similar overall trends were observed for both specimen types. Additionally, to verify that the fibers were completely removed according to the proposed modified burn-off test procedure, each specimen was subjected to at least three additional heating and mass measurement cycles after the mass had reached an apparent stable state with no further weight change. These results confirmed that no additional mass loss occurred and that the mass remained stable throughout the repeated measurements. For all specimens, no further weight change was detected during these repeated cycles, indicating that errors due to partially pyrolyzed fiber residues were negligible. Notably, for specimens with greater thickness and weight, the time to weight stability with no further changes was longer. Additionally, the total testing time was longer for the flax specimens than for the hemp specimens. This was attributed to the lower burn-off temperature used for the flax and the larger size of the flax specimens. The final *Gc* values derived from the modified burn-off tests for the hemp and flax specimens are summarized in Tables 12 and 13, respectively. These values were calculated using Eq. (4) based solely on the weight of the resin remaining after the complete combustion of the natural fibers.

These results indicate that the *Gc* values for hemp and flax specimens

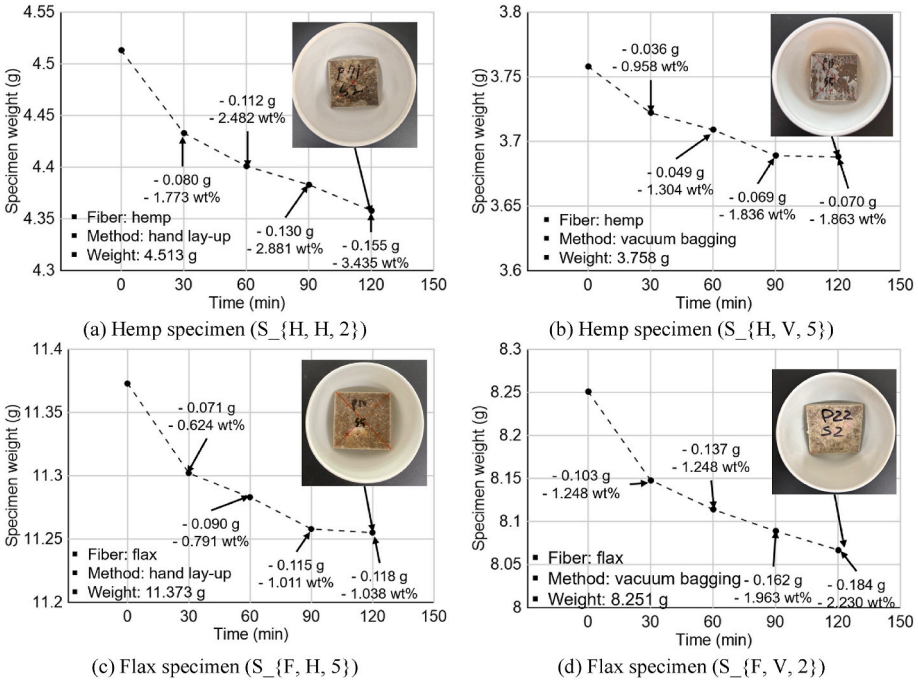

Fig. 7. Examples of pre-heating results for selected hemp and flax composite specimens.

Table 10
Weights and relative densities of the hemp specimens before and after pre-heating and *Gc* values measured after pre-heating.

Specimen	Before pre-heating		After pre-heating		*Gc* (wt%) (Method IV)
	Weight (g)	Relative density (g/cm^3)	Weight (g)	Relative density (g/cm^3)	
S_{H, H, 1}	4.685	1.07	4.571	1.06	42.235
S_{H, H, 2}	4.513	1.07	4.358	1.05	43.621
S_{H, H, 4}	4.734	1.06	4.559	1.05	40.977
S_{H, H, 5}	4.619	1.06	4.452	1.04	42.935
S_{H, H, 6}	4.559	1.06	4.391	1.04	43.290
S_{H, V, 2}	3.870	1.15	3.800	1.13	37.400
S_{H, V, 3}	3.778	1.16	3.726	1.15	38.745
S_{H, V, 4}	3.780	1.15	3.716	1.13	38.921
S_{H, V, 5}	3.758	1.15	3.688	1.14	39.115

Table 11
Weights and relative densities of the flax specimens before and after pre-heating and *Gc* values measured after pre-heating.

Specimen	Before pre-heating		After pre-heating		*Gc* (wt%) (Method IV)
	Weight (g)	Relative density (g/cm^3)	Weight (g)	Relative density (g/cm^3)	
S_{F, H, 1}	11.011	1.06	10.906	1.05	16.215
S_{F, H, 2}	9.953	1.06	9.862	1.05	17.885
S_{F, H, 3}	10.255	1.03	10.150	1.02	17.148
S_{F, H, 4}	10.562	1.03	10.413	1.01	16.476
S_{F, H, 5}	11.373	1.06	11.255	1.05	15.616
S_{F, H, 6}	10.354	1.07	10.245	1.05	17.122
S_{F, V, 1}	9.052	0.95	8.902	0.93	24.542
S_{F, V, 2}	8.251	0.92	8.067	0.91	26.174
S_{F, V, 3}	8.026	0.88	7.791	0.86	26.584
S_{F, V, 4}	8.020	0.86	7.698	0.83	26.050
S_{F, V, 5}	8.256	0.87	7.972	0.86	25.803

fabricated using the same manufacturing process were generally comparable. However, specimen S_{F, V, 1} exhibited a relatively higher *Gc* value compared with other specimens produced under identical fabrication conditions. For specimen S_{F, V, 1}, no visible defects or surface abnormalities were observed during post-fabrication visual inspection. Nevertheless, it exhibited an initial mass approximately 1 g greater than that of other specimens of similar size, along with a relatively higher measured density (Fig. 6). These observations suggest that specimen S_{F, V, 1} may have contained additional material with a density and mass comparable to those of flax fibers, in addition to the flax fiber and epoxy resin. During the modified burn-off test, such material would have been removed along with the flax fibers, leading to a larger measured amount of combusted reinforcement and, consequently, a higher calculated *Gc* value compared with other specimens. This occurrence reflects a common issue that can arise during fiber-reinforced composite fabrication. Moreover, it highlights the need for burn-off-test-based verification to accurately determine the constituent composition of fiber-reinforced composites.

Fig. 10 summarizes the void volume content, or internal defects, measured in the hemp and flax specimens using Eq. (5). Compared to FRP laminates that typically use glass fiber, the NFRP laminates exhibited higher void volumes [9,58]. This finding underscores the importance of evaluating laminate quality when considering NFRP application in ship structures.

6. Discussion

In this study, the modified burn-off method for *Gc* and internal defect measurement was adjusted for the inherent characteristics of natural fibers. To verify the reliability of the modified method, a comparative analysis was performed with other *Gc* measurement methods for a general FRP ship structure. The methods considered were as follows: rule calculation, which is typically applied to FRP ship structures; direct measurement; direct measurement using a hydrometer; direct measurement with pre-heating to reflect the natural fiber characteristics; and the modified burn-off test. In this section, the *Gc* results obtained from these different methods are compared and analyzed. Additionally, the effects of the moisture absorbed by natural fibers are discussed, and the internal defects of natural fiber composites are compared with those of conventional GFRPs.

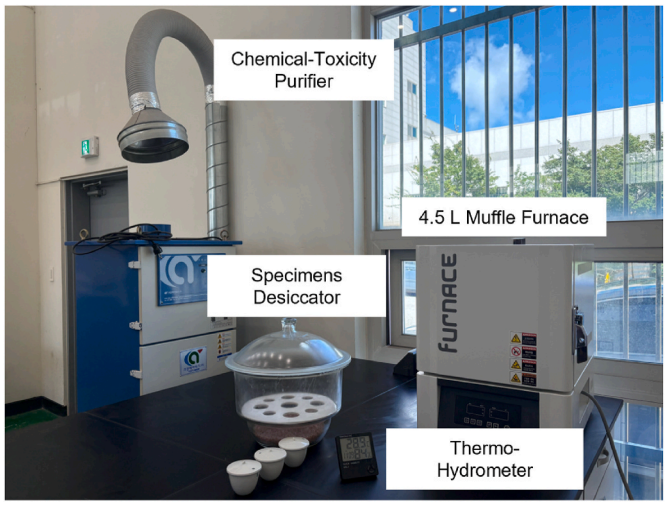

Fig. 8. Experimental setup for the modified burn-off test.

6.1. Comparison between the conventional ship-structure Gc measurement and the proposed modified burn-off method

This section reports the comparison between the *Gc* values for the hemp and flax composites obtained using the five aforementioned methods. Prior to comparison, a boxplot analysis was conducted using the results from the modified burn-off test, as shown in Fig. 11. Outlier detection was performed using an interquartile range (IQR)-based approach. Considering the small sample size, coefficient *k* was conservatively set to 0.85 for a stricter outlier identification criterion. Consequently, specimen S1 among the flax hand-lay-up specimens and specimen S1 among the vacuum bagged specimens were identified as outliers and excluded from the subsequent analysis.

Across all methods, consistent trends were observed for the *Gc* results regardless of fiber type. First, a comparison between Methods I and II revealed discrepancies between the design-based and fabricated specimens, indicating that such variation is inherent in composite materials. This result highlights the importance of verifying the fabricated *Gc* to ensure structural safety for shipbuilding applications. Next, a comparison between Methods II and III revealed a slight decrease in *Gc* across all groups. This can be attributed to dimensional measurement errors, as shown in Fig. 12, in which rough edges in the NFRP specimens (which were present despite precise cutting) introduced deviations. These findings suggest that use of a hydrometer to determine the relative density of the specimen enables more accurate *Gc* measurements.

A comparison between Methods III and IV revealed a further decrease in *Gc* after pre-heating. This was due to absorbed moisture removal from within the fibers and indicates that the pre-heating process effectively corrected the *Gc* values that were previously affected by moisture. These results underscore the need for a pre-heating step for accurate *Gc* measurements in NFRP composites. Finally, a comparison between Methods IV and V revealed an additional decrease in *Gc*. This decline was interpreted as being due to the internal defects present in the NFRP specimens, which were reflected in the modified burn-off test.

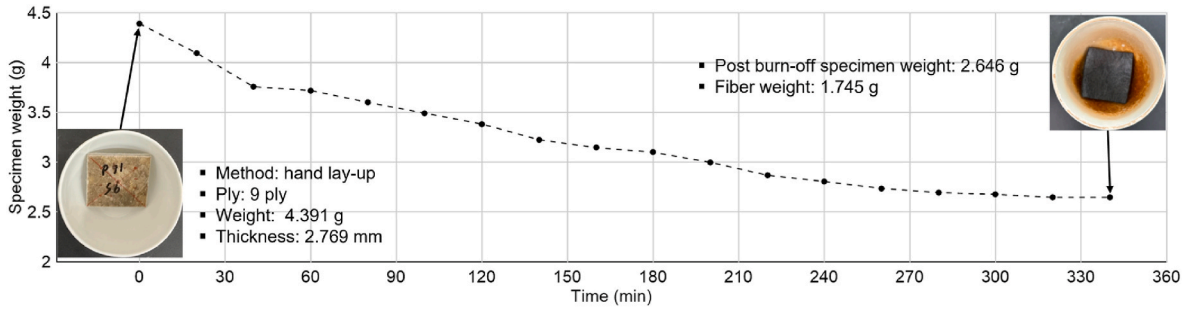

(a) Hemp specimen (S_{H, H, 6})

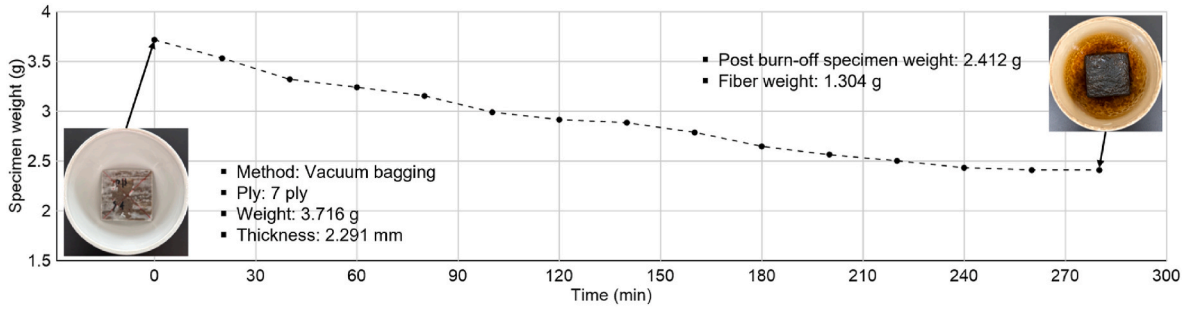

(b) Hemp specimen (S_{H, V, 4})

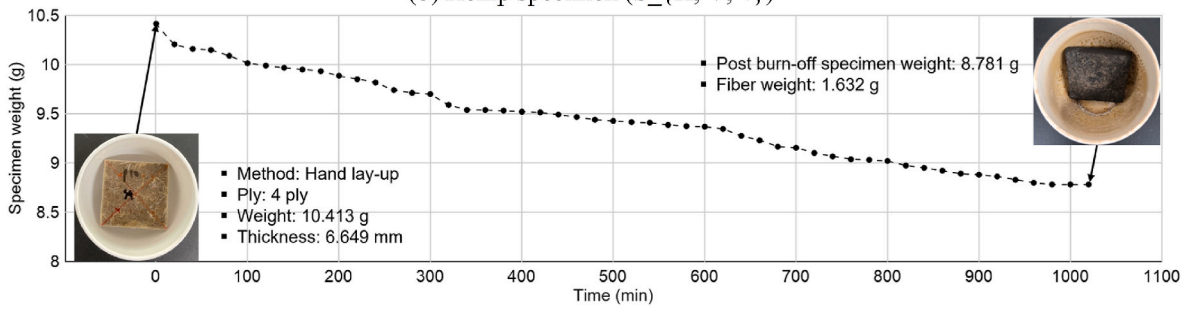

(c) Flax specimen (S_{F, H, 4})

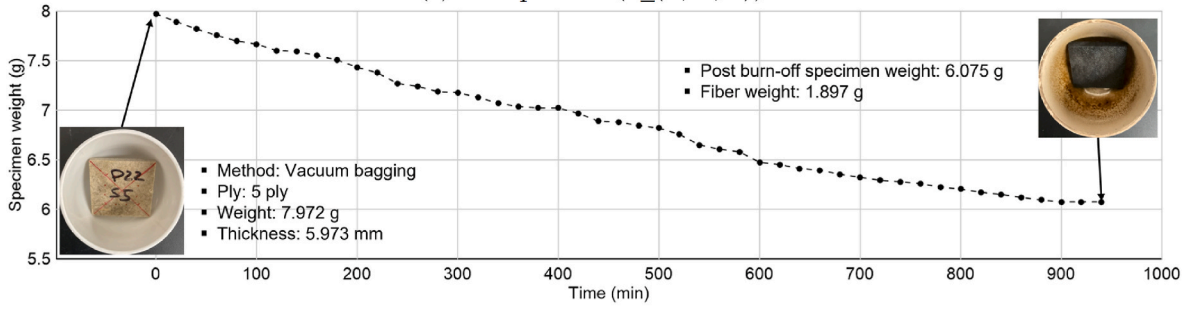

(d) Flax specimen (S_{F, V, 5})

Fig. 9. Examples of weight change trends observed during the modified burn-off test for selected NFRP specimens.

6.2. Analysis of the effectiveness of pre-heating in addressing moisture absorption in natural fibers

To determine whether the moisture removed during the pre-heating process was statistically significant, a statistical analysis was conducted. Specifically, a paired *t*-test was used to compare the differences before and after pre-heating. Unlike a general *t*-test, the paired *t*-test evaluates the difference in means within the same group before and after a particular event, focusing on paired data. The analysis was conducted separately for four groups: hemp hand-lay-up specimens, hemp vacuum-bagging specimens, flax hand-lay-up specimens, and flax vacuum-bagging specimens. Minitab software [94] was used for the analysis. Prior to the main analysis, normality of the differences between each pair—an assumption in the paired t-test—was verified and satisfied for all groups. These results are presented in Fig. 13.

For the hemp hand-lay-up and vacuum-bagging specimens, the *p*-values were 1.41E-04 and 6.32E-04, respectively. For the flax hand-lay-up and vacuum-bagging groups, the *p*-values were 2.94E-04 and 0.003, respectively. Therefore, in all cases, the weight change caused by moisture removal during pre-heating was statistically significant (see Table 14). These findings confirm that moisture absorption in natural fibers is a crucial factor. Therefore, the proposed pre-heating step is essential for obtaining accurate *Gc* measurements in NFRP composites.

Table 12
Gc measurement results for the hemp specimens obtained using the modified burn-off method.

Specimen	Specimen weight (g)	Post-burn-off resin weight (g)	Calculated fiber weight (g)	*Gc* (wt%) (Method V)
S_{H, H, 1}	4.571	2.570	2.001	43.776
S_{H, H, 2}	4.358	2.522	1.836	42.129
S_{H, H, 4}	4.559	2.258	2.301	50.472
S_{H, H, 5}	4.452	2.564	1.888	42.408
S_{H, H, 6}	4.391	2.646	1.745	39.740
S_{H, V, 2}	3.800	2.432	1.368	36.000
S_{H, V, 3}	3.726	2.351	1.375	36.903
S_{H, V, 4}	3.716	2.412	1.304	35.091
S_{H, V, 5}	3.688	2.207	1.481	40.157

Table 13
Gc measurement results for the flax specimens obtained using the modified burn-off method.

Specimen	Specimen weight (g)	Post-burn-off resin weight (g)	Calculated fiber weight (g)	*Gc* (wt%) (Method V)
S_{F, H, 1}	10.906	8.626	2.644	24.244
S_{F, H, 2}	9.862	8.345	1.517	15.382
S_{F, H, 3}	10.150	8.536	1.614	15.901
S_{F, H, 4}	10.413	8.781	1.632	15.673
S_{F, H, 5}	11.255	9.559	1.696	15.069
S_{F, H, 6}	10.245	8.485	1.655	16.252
S_{F, V, 1}	8.902	3.741	5.161	57.976
S_{F, V, 2}	8.067	6.178	1.889	23.416
S_{F, V, 3}	7.791	5.789	2.002	25.696
S_{F, V, 4}	7.698	5.681	2.017	26.202
S_{F, V, 5}	7.972	6.075	1.897	23.796

6.3. Comparative analysis between NFRP and conventional GFRP quality

This section reports a quality comparison between the NFRP specimens and GFRP laminates, which are commonly used in ship structures. The results are presented in Fig. 14. For hand-lay-up GFRP specimens, Han et al. [58] reported void contents of approximately 0.95% and 1.20% for low- and high-*Gc* laminates, respectively. By contrast, average void contents of 14.782% and 5.847% were obtained in this study for the hemp hand-lay-up and vacuum-bagging specimens, respectively. For the flax hand-lay-up and vacuum-bagging specimens, the values were 9.552% and 26.059%, respectively. Based on these results, the NFRP laminates exhibited a general tendency toward increased internal defects compared to the GFRP laminates, with differences ranging between approximately five- and twenty-fold on average. However, considering the variability arising from differences in material properties and manufacturing characteristics between the two experiments, these results should be interpreted in terms of the relative trend rather than the absolute magnitude ratio. This disparity can be attributed to the inherent moisture content of natural fibers. Moisture reduces the interfacial bonding strength between the hydrophilic natural fiber and hydrophobic polymer resin, causing void formation [40,79]. Additionally, the hygroscopic nature and heterogeneous microstructure of natural fibers often lead to insufficient resin impregnation, which further contributes to void generation within the fiber bundles and at the fiber–matrix interface [95]. Furthermore, as such internal defects can significantly impact structural integrity, they must be assessed and minimized when NFRP materials are applied to ship structures.

7. Conclusion

The structural strength of FRP marine structures is fundamentally determined by the reinforcing fiber, and the estimation of that strength relies on the fiber content (*Gc*). Thus, accurate *Gc* measurement is crucial for the effective design and safety validation of ship structures. This study examined existing methods for *Gc* and internal defect measurement of NFRPs and identified the limitations of the conventional burn-off method, which, despite its high accuracy, is difficult to apply to NFRPs. Based on the results, a modified burn-off method suitable for NFRPs is proposed. The proposed method considers the unique characteristics of natural fibers, including their high moisture absorption and low ignition point, by incorporating a pre-heating step and adjusting the burn temperature.

Unlike conventional resin burn-off-based methods, the proposed approach selectively combusts the natural fibers and directly quantifies the remaining resin mass, thereby enabling quantitative evaluation of the constituent composition and internal void content of NFRPs. The proposed method was applied to specimens fabricated with actual hemp and flax fibers, demonstrating consistent and repeatable results in terms of both *Gc* and void measurements. The validity of the proposed method was demonstrated through comparisons with standard *Gc* measurement techniques.

The rule calculation method enabled fast and simple *Gc* estimation based on theoretical equations. However, noticeable deviations were observed when the results were compared to values measured from actual fabricated specimens. The direct measurement method proved more accurate when a hydrometer was employed, as this device enabled more precise dimensional assessment of the specimens. Though pre-heating and hydrometer-based measurements, the amount of moisture was confirmed to be 2.623 $\pm$ 0.976 and 1.877 $\pm$ 1.115 wt% for the hemp- and flax-fiber specimens, respectively. The results converge to a specific value during the experiment and exhibited values similar to those reported in the literature. This verifies that the determined test condition for pre-heating (70 °C; 2 h) was suitable. Furthermore, it was statistically confirmed that the added pre-heating step can correct *Gc* measurement errors due to moisture from the natural fibers. Thus, it can be concluded that pre-heating is an essential procedure for *Gc* measurements of NFRP composite materials. Additionally, the proposed modified burn-off method can verify the internal defects of NFRPs quantitatively. Compared to conventional GFRPs, a void content exceeding a factor of 20 was found in NFRPs, primarily because of the weakened interfacial bonding strength due to the moisture from the natural fibers. Additionally, the hygroscopic nature and heterogeneous microstructure of natural fibers often lead to insufficient resin impregnation, which further contributes to void generation within the fiber bundles and at the fiber–matrix interface.

The results of this study confirm that the proposed modified burn-off method is applicable to hemp- and flax-based NFRPs, and demonstrate that accurate *Gc* and internal defect evaluation is essential for the safe application of NFRPs in ship structures. Despite these advantages, several limitations regarding the proposed approach were identified. First, while the proposed method is considered applicable to general NFRP systems, additional verification of the appropriate test temperature range is required, as the thermal degradation behavior may vary according to the specific natural fiber and epoxy resin employed. Second, although the proposed method is expected to be applicable to thicker laminates representative of actual ship structures, further consideration of test conditions—such as the increased time required for mass stabilization during the modified burn-off process—is needed. Additionally, for hybrid composites composed of synthetic and natural fibers, which have been actively studied in recent years, the proposed modified burn-off test could be applicable if the constituent materials are selectively combusted in sequence, namely, the natural fibers followed by the resin. However, in the case of hybrid composites, the introduction of additional combustion stages would inevitably increase the testing procedure complexity, and further verification of the influence of the experimental duration at each stage is required. Therefore, further research is needed to investigate the correlations among accurately measured *Gc*, internal defects, and mechanical properties based on the proposed method. Furthermore, the development of hull

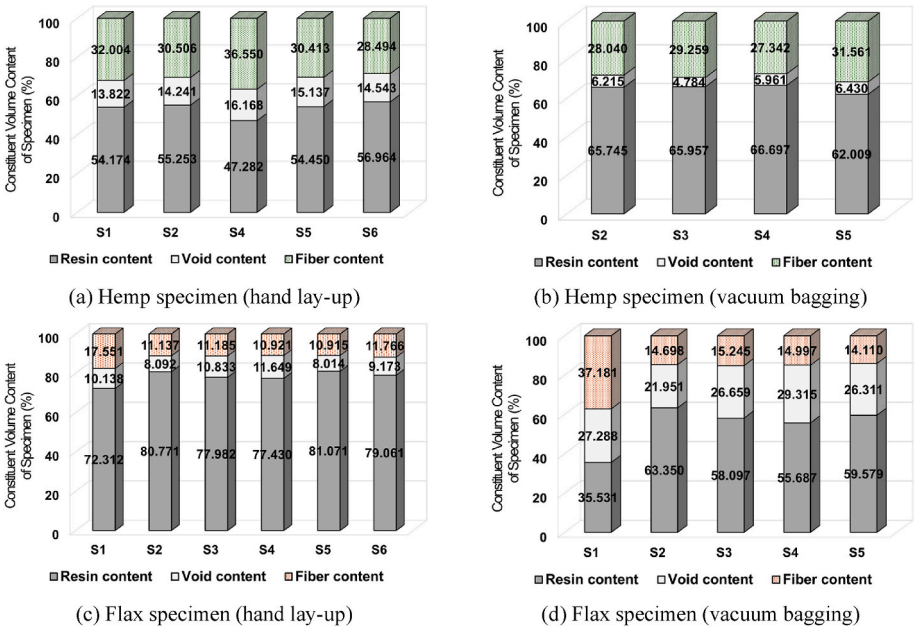

Fig. 10. Void volume contents of NFRP specimens measured using the modified burn-off test.

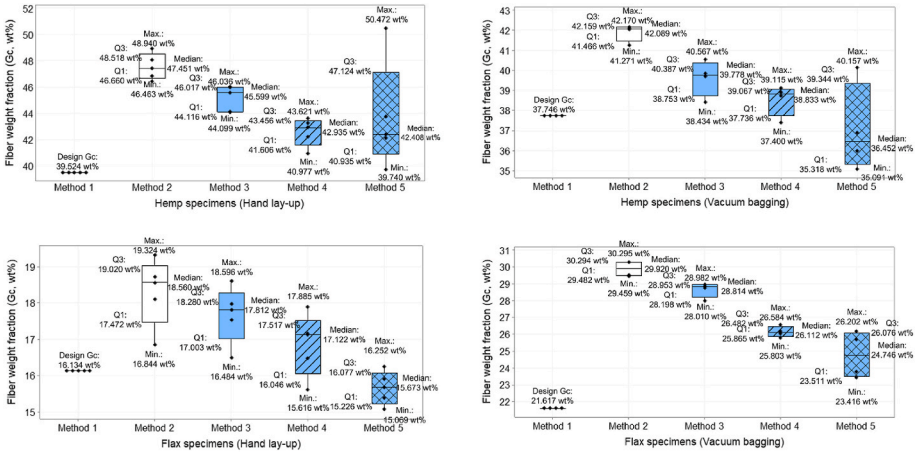

Fig. 11. *Gc* measurement results for the hemp and flax specimens according to fabrication method.

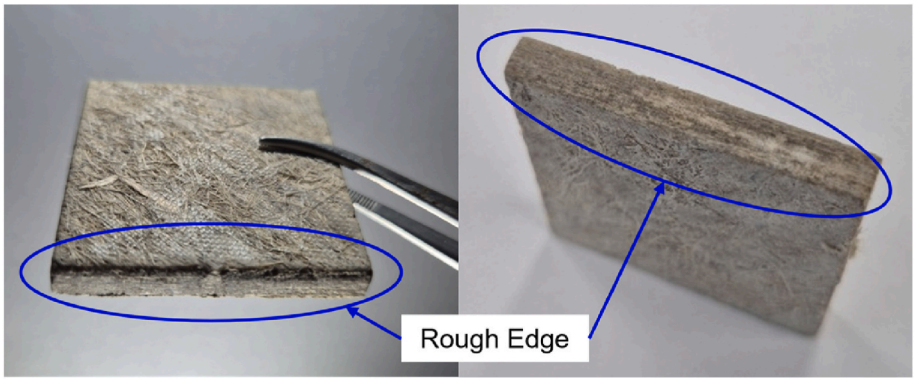

Fig. 12. Rough edges observed in selected hemp specimens.

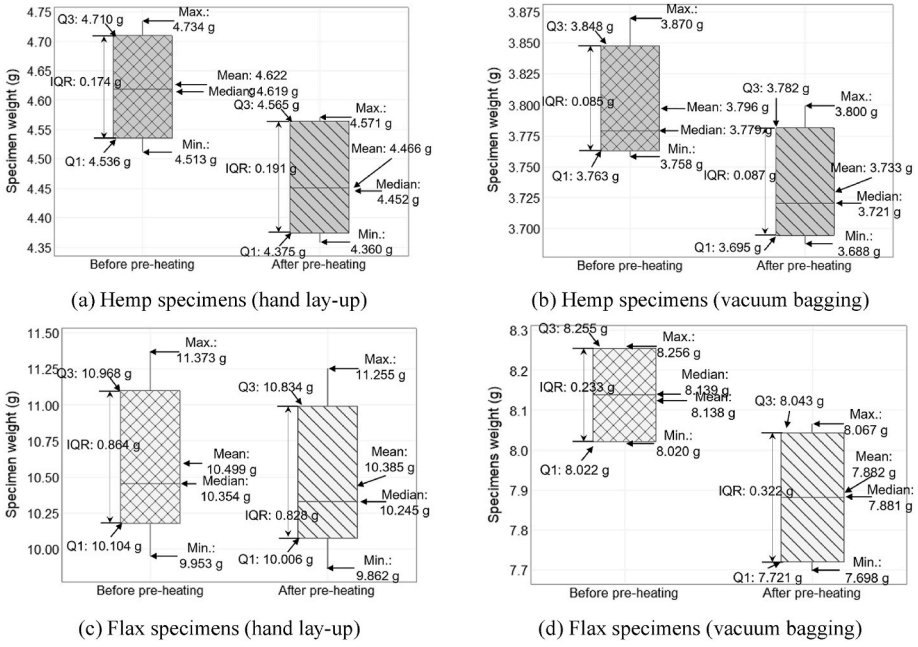

Fig. 13. Paired *t*-test results for moisture absorption in the NFRP specimens.

Table 14
Paired *t*-test results for moisture absorption in the NFRP specimens.

Fiber	Method	Pre-heating	Sample size	Mean specimen weight (g)	St. dev.	SE mean	Effect size	*p*-value
Hemp	Hand lay-up	Before	5	4.622	0.090	0.040	6.492	1.41E-04
		After	5	4.466	0.096	0.043		
	Vacuum bagging	Before	4	3.796	0.050	0.025	8.000	6.32E-04
		After	4	3.733	0.048	0.024		
Flax	Hand lay-up	Before	5	10.499	0.535	0.239	5.200	2.94E-04
		After	5	10.385	0.526	0.235		
	Vacuum bagging	Before	4	8.138	0.133	0.067	4.271	0.003
		After	4	7.882	0.168	0.084		

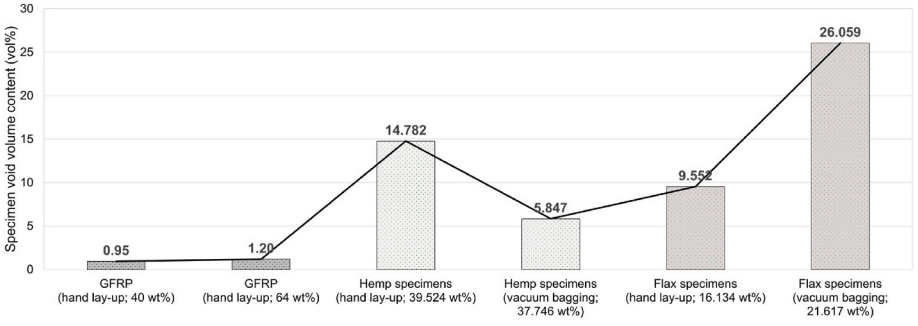

Fig. 14. Internal defect comparison between the GFRP and NFRP specimens [58].

structural design criteria and material property prediction models for NFRPs that incorporate these relationships is expected to be an important research direction for advancing NFRP application in marine structures.

Funding

This work was supported by the Oceans and Fisheries Department of the Korean Government through the "Development of Technologies to Improve Passenger Ship Efficiency based on Renewable Energy" project [grant number RS-2022-KS221551/PMS6370] and the Lloyd's Register Foundation under grant Sg8/100079 for the "Safe and Sustainable Composite Yacht and Ship Structures" project.

CRediT authorship contribution statement

Jaewon Jang: Conceptualization, Data curation, Formal analysis, Investigation, Methodology, Visualization, Writing – original draft. **Jean-Baptiste R.G. Souppez:** Conceptualization, Data curation, Funding acquisition, Methodology, Validation, Writing – review & editing. **Daekyun Oh:** Conceptualization, Data curation, Funding acquisition, Methodology, Project administration, Writing – review & editing.

Declaration of competing interest

The authors declare that they have no known competing financial interests or personal relationships that could have appeared to influence

the work reported in this paper.

Acknowledgements

The authors gratefully acknowledge the support of Lloyd's Register, UK. The authors also acknowledge that the leadership and insight provided through the role of the ISO/TC 188/WG 35 Convenor significantly inspired and informed the conceptual foundation of this research.

Data availability

Data will be made available on request.

References

[1] N. Han, J. Song, J. Jang, J. Noh, Z. Han, D. Oh, Lightweight deep learning neural networks for analyzing infrared thermal imaging non-destructive inspection results, Trans. Korean Soc. Mech. Eng. A 48 (2024) 671–680, https://doi.org/10.3795/KSME-A.2024.48.10.671.

[2] M. Zhang, Q. Chen, J. Zhuo, Y. Cai, Z. Zhu, X. Li, M. Peng, K. Fan, Y. Qin, Machine learning-based optimization of impact-resistant layups for FRP hybrid laminates in yachts, Ocean Eng. 324 (1) (2025) 120600, https://doi.org/10.1016/j.oceaneng.2025.120600.

[3] M.P.M. Dicker, P.F. Duckworth, A.B. Baker, G. Francois, M.K. Hazzard, P. M. Weaver, Green composites: a review of material attributes and complementary applications, Compos. Part A Appl. Sci. Manuf. 56 (2014) 280–289, https://doi.org/10.1016/j.compositesa.2013.10.014.

[4] G. Fredi, A. Dorigato, L. Fambri, S.H. Unterberger, A. Pegoretti, Effect of phase change microcapsules on the thermo-mechanical, fracture and heat storage properties of unidirectional carbon/epoxy laminates, Polym. Test. 91 (2020) 106747, https://doi.org/10.1016/j.polymertesting.2020.106747.

[5] S. Saha, S. Kumar, V.K. Mahakur, S. Sharma, A. Saha, Development and machine learning based prediction of carbon/hemp/ramie sandwich composite as sustainable and ecofriendly solution for automobile application, Mater. Today Commun. 41 (2024) 110817, https://doi.org/10.1016/j.mtcomm.2024.110817.

[6] Innopolis Korea Innovation Foundation, Composites market. pp. 1-18. https://www.innopolis.or.kr/board/view?linkId=44436&menuId=MENU00999 (accessed 21 July 2025).

[7] A. Saha, P. Kumari, Functional fibers from Bambusa tulda (Northeast Indian species) and their potential for reinforcing biocomposites, Mater. Today Commun. 31 (2022) 103800, https://doi.org/10.1016/j.mtcomm.2022.103800.

[8] A. Saha, N.D. Kulkarni, P. Kumari, Development of Bambusa tulda fiber-micro particle reinforced hybrid green composite: a sustainable solution for tomorrow's challenges in construction and building engineering, Constr. Build. Mater. 441 (2024) 137486, https://doi.org/10.1016/j.conbuildmat.2024.137486.

[9] J. Jang, Maydison, Y. Kim, Z. Han, D. Oh, Effect of void content on the mechanical properties of GFRP for ship design, J. Mar. Sci. Eng. 11 (2023) 1251, https://doi.org/10.3390/jmse11061251.

[10] M.J. Lowde, H.G.A. Peters, R. Geraghty, J. Graham-Jones, R. Pemberton, J. Summerscales, The 100 m composite ship? J. Mar. Sci. Eng. 10 (3) (2022) 408, https://doi.org/10.3390/jmse10030408.

[11] Y. Wang, M. Wang, C. Zheng, L. Yang, H. Zhang, Y. Li, X. Ruan, Experimental investigation of slamming impact on fiber-reinforced composite sandwich bow structure, Ocean Eng. 319 (2025) 120162, https://doi.org/10.1016/j.oceaneng.2024.120162.

[12] The Society of Naval Architects of Korea Webzine, Marine composites, FRP small craft, and eco-friendliness. http://www.snak.or.kr/newsletter/webzine/news.html?Item=board21&mode=view&s_t=1&No=645. (Accessed 21 July 2025).

[13] S.J. Pickering, Recycling technologies for thermoset composite materials – current status, Compos. Part A Appl. Sci. Manuf. 37 (2006) 1206–1215, https://doi.org/10.1016/j.compositesa.2005.05.030.

[14] J.C. Gerdeen, H.W. Lord, R.A.L. Rorrer, Engineering Design with Polymers and Composites, first ed., CRC Press, Boca Raton, 2006.

[15] R. Hao, S. Xue, H. Sun, T. Yang, H. Wang, Emission characteristics and the environmental impact of VOCs from typical FRP manufacture industry, Atmos 13 (2022) 1274, https://doi.org/10.3390/atmos13081274.

[16] Y.F. Khalil, Eco-efficient lightweight carbon-fiber reinforced polymer for environmentally greener commercial aviation industry, Sustain. Prod. Consum. 12 (2017) 16–26. https://www.sciencedirect.com/science/article/pii/S2352550917300179.

[17] A.U. Zaman, S.A. Gutub, M.F. Soliman, M.A. Wafa, Sustainability and human health issues pertinent to fibre reinforced polymer composites usage: a review, J. Reinforc. Plast. Compos. 33 (2014) 1069–1084. https://journals.sagepub.com/doi/10.1177/0731684414521087.

[18] R. Frassine, C. Fusaro, A. Ratti, Chemical hazard in FRP pleasure boat's manufacturing, in: N. Stanton, S. Landry, G. Di Bucchianico, A. Vallicelli (Eds.), Advances in Human Aspects of Transportation: Part I, AHFE International, U.S.A., 2021, pp. 171–179. https://books.google.co.kr/books?hl=en&id=O3xYBAAAQBAJ&pg=PA171#v=onepage&q&f=false.

[19] Jiangsu Zeyusen Carbon Fiber Technology, Impact of glass fiber cloth on the environment. https://www.jsfiberglass.com/news/industry-news/impact-of-glass-fiber-cloth-on-the-environment.html. (Accessed 21 July 2025).

[20] ANGUIL, New clean air techniques for carbon fiber processes, in: https://anguil.com/news/new-clean-air-techniques-for-carbon-fiber-processes/. (Accessed 21 July 2025).

[21] S. Kumar, A. Saha, Utilization of coconut shell biomass residue to develop sustainable biocomposites and characterize the physical, mechanical, thermal, and water absorption properties, Biomass Convers. Biorefinery 14 (2024) 12815–12831, https://doi.org/10.1007/s13399-022-03293-4.

[22] European Parliament, Directive 2000/53/EC of the council of 18 September 2000 on end-of life vehicles, O.J. (L 269), 34 – 43, https://eur-lex.europa.eu/eli/dir/2000/53/oj/eng, 2000.

[23] International Maritime Organization, The Hong Kong international convention for the safe and environmentally sound recycling of ships. https://www.imo.org/en/about/conventions/pages/the-hong-kong-international-convention-for-the-safe-and-environmentally-sound-recycling-of-ships.aspx. (Accessed 21 July 2025).

[24] European Parliament, Regulation (EU) no 1257/2013 of the council of 20 November 2013 on ship recycling and amending regulation (EC) no 1013/2006 and directive 2009/16/EC, 2013 O.J. (L 330, 1 – 20, https://eur-lex.europa.eu/legal-content/EN/TXT/?uri=CELEX%3A32013R1257.

[25] J. Summerscales, M.M. Singh, K. Wittamore, Disposal of composite boats and other marine composites, in: J. Graham-Jones, J. Summerscales (Eds.), Marine Applications of Advanced Fibre-Reinforced Composites, Woodhead Publishing, Cambridge, 2016, pp. 185–213. https://www.sciencedirect.com/science/article/abs/pii/B9781782422501000089.

[26] G. Oliveux, L.O. Dandy, G.A. Leeke, Current status of recycling of fibre reinforced polymers: review of technologies, reuse and resulting properties, Prog. Mater. Sci. 72 (2015) 61–99, https://doi.org/10.1016/j.pmatsci.2015.01.004.

[27] K. Kawajiri, M. Kobayashi, Cradle-to-Gate life cycle assessment of recycling processes for carbon fibers: a case study of ex-ante life cycle assessment for commercially feasible pyrolysis and solvolysis approaches, J. Clean. Prod. 378 (2022) 134581, https://doi.org/10.1016/j.jclepro.2022.134581.

[28] A.E. Krauklis, C.W. Karl, A.I. Gagani, J.K. Jørgensen, Composite material recycling technology—State-of-the-art and sustainable development for the 2020s, J. Compos. Sci. 5 (2021) 28, https://doi.org/10.3390/jcs5010028.

[29] J.-B.R.G. Souppez, G.S. Pavar, Recycled carbon fibre composites in automotive manufacturing, Int. J. Automoto. Manuf. Mater. 2 (1) (2023) 1–12, https://doi.org/10.53941/ijamm0201003.

[30] Z. Han, J. Jang, J.-B.R.G. Souppez, Maydison, D. Oh, Environmental implications of a sandwich structure of a glass fiber-reinforced polymer ship, Ocean Eng. 298 (2024) 117122, https://doi.org/10.1016/j.oceaneng.2024.117122.

[31] Q. Hou, Life cycle assessment of cruising ship superstructure [bachelor's thesis], Institutionen för geovetenskaper, Uppsala, 2011. http://www.diva-portal.org/smash/get/diva2:451090/FULLTEXT01.pdf.

[32] S. Karbalaei, P. Hanachi, T.R. Walker, M. Cole, Occurrence, sources, human health impacts and mitigation of microplastic pollution, Environ. Sci. Pollut. Res. 25 (2018) 36046–36063, https://doi.org/10.1007/s11356-018-3508-7.

[33] S. Castegnaro, C. Gomiero, C. Battisti, M. Poli, M. Basile, P. Barucco, U. Pizzarello, M. Quaresimin, A. Lazzaretto, A bio-composite racing sailboat: materials selection, design, manufacturing and sailing, Ocean Eng. 133 (2017) 142–150, https://doi.org/10.1016/j.oceaneng.2017.01.017.

[34] A. Le Duigou, A. Bourmaud, P. Davies, C. Baley, Long term immersion in natural seawater of Flax/PLA biocomposite, Ocean Eng. 90 (2014) 140–148, https://doi.org/10.1016/j.oceaneng.2014.07.021.

[35] C.-N. Bae, S.-Y. Hwang, J.-H. Lee, U.-C. Jeong, K.-H. Kim, Multi point press forming system applied to curved hull plate of aluminum ship, Trans. Soc. CAD/CAM Eng. 17 (2012) 188–197, https://doi.org/10.7315/CADCAM.2012.188.

[36] D.-H. Cho, H.-J. Kim, Naturally cyclable biocomposites, Elastomers Compos. 44 (1) (2009) 13–21. https://koreascience.kr/article/JAKO200912651520750.page.

[37] A. Saha, N.D. Kulkarni, P. Kumari, Development of bambusa tulda-reinforced different biopolymer matrix green composites and MCDM-based sustainable material selection for automobile applications, Environ. Dev. Sustain. 27 (2025) 10655–10691, https://doi.org/10.1007/s10668-023-04327-1.

[38] A. Saha, P. Kumari, Effect of alkaline treatment on physical, structural, mechanical and thermal properties of Bambusa tulda (Northeast Indian species) based sustainable green composites, Polym. Compos. 44 (2023) 2449–2473, https://doi.org/10.1002/pc.27256.

[39] A. Arbelaiz, G. Cantero, B. Fernandez, I. Mondragon, P. Gañán, J.M. Kenny, Flax fiber surface modifications: effects on fiber physico mechanical and flax/polypropylene interface properties, Polym. Compos. 26 (3) (2005) 324–332, https://doi.org/10.1002/pc.20097.

[40] Y. Li, K.L. Pickering, Hemp fibre reinforced composites using chelator and enzyme treatments, Compos. Sci. Technol. 68 (2008) 3293–3328, https://doi.org/10.1016/j.compscitech.2008.08.022.

[41] R. Malkapuram, V. Kumar, Y.S. Negi, Recent development in natural fiber reinforced polypropylene composites, J. Reinforc. Plast. Compos. 28 (2008) 1169–1189, https://doi.org/10.1177/0731684407087759.

[42] M. Mohammed, A.J.M. Jawad, A. Mohammed, J.K. Oleiwi, T. Adam, A.F. Osman, O.S. Dahham, B.O. Betar, S.C.B. Gopinath, M. Jaafar, Challenges and advancement in water absorption of natural fiber-reinforced polymer composites, Polym. Test. 124 (2023) 108083, https://doi.org/10.1016/j.polymertesting.2023.108083.

[43] G. Bogoeva-Gaceva, M. Avella, M. Malinconico, A. Buzarovska, A. Grozdanov, G. Gentile, M.E. Errico, Natural fiber eco-composites, Polym. Compos. 28 (2007) 98–107, https://doi.org/10.1002/pc.20270.

[44] A.N. Fraga, E. Frullloni, O.D.L. Osa, J.M. Kenny, A. Vázquez, Relationship between water absorption and dielectric behaviour of natural fibre composite materials, Polym. Test. 25 (2006) 181–187, https://doi.org/10.1016/j.polymertesting.2005.11.002.

[45] A. Wang, X. Wang, G. Xian, The influence of stacking sequence on the low-velocity impact response and damping behavior of carbon and flax fabric reinforced hybrid composites, Polym. Test. 104 (2021) 107384, https://doi.org/10.1016/j.polymertesting.2021.107384.

[46] B. Koohestani, A.K. Darban, P. Mokhtari, E. Yilmaz, E. Darezereshki, Comparison of different natural fiber treatments: a literature review, Int. J. Environ. Sci. Technol. 16 (2019) 629–642, https://doi.org/10.1007/s13762-018-1890-9.

[47] S. Islam, F.E. Karim, R. Islam, Assessing the consequences of water retention on the structural integrity of jute fiber and its composites: a review, SPE Polym 5 (2024) 457–480, https://doi.org/10.1002/pls2.10142.

[48] S. Islam, B. Hasan, An overview of the effects of water and moisture absorption on the performance of hemp fiber and its composites, SPE Polym 6 (2024) e10167, https://doi.org/10.1002/pls2.10167.

[49] P.F. Alao, L. Marrot, H. Kallakas, A. Just, T. Poltimäe, J. Kers, Effect of hemp fiber surface treatment on the moisture/water resistance and reaction to fire of reinforced PLA composites, Mater 14 (2021) 4332, https://doi.org/10.3390/ma14154332.

[50] M.S. Islam, K.L. Pickering, N.J. Foreman, Influence of hygrothermal ageing on the physico-mechanical properties of alkali treated industrial hemp fibre reinforced polylactic acid composites, J. Polym. Environ. 18 (2010) 696–704, https://doi.org/10.1007/s10924-010-0225-9.

[51] S. Luo, A.N. Netravali, Mechanical and thermal properties of environment-friendly ‘‘green’’ composites made from pineapple leaf fibers and poly(hydroxybutyrate-co-valerate) resin, Polym. Compos. 20 (3) (1999) 367–378, https://doi.org/10.1002/pc.10363.

[52] I. Rácz, H. Hargitai, Influence of water on properties of cellulosic fibre reinforced polypropylene composites, Int. J. Polym. Mater. Polym. Biomater. 47 (2000) 667–674, https://doi.org/10.1080/00914030008031321.

[53] S. Mishra, J.B. Naik, Y.P. Patil, The compatibilising effect of maleic anhydride on swelling and mechanical properties of plant-fibre-reinforced novolac composites, Compos. Sci. Technol. 60 (2000) 1729–1735, https://doi.org/10.1016/S0266-3538(00)00056-7.

[54] A.E. Faola, I.O. Oladele, B.O. Adewuyi, K.E. Oluwabunmi, Effect of chemical treatment on water absorption capability of polyester composite reinforced with particulate agro-fibres, Chem. Mater. Res. 3 (2013) 106–112. https://core.ac.uk/download/pdf/234666311.pdf.

[55] Y. Chen, N. Su, K. Zhang, S. Zhu, Z. Zhu, W. Qin, et al., Effect of fiber surface treatment on structure, moisture absorption and mechanical properties of luffa sponge fiber bundles, Ind. Crops Prod. 123 (2018) 341–352, https://doi.org/10.1016/j.indcrop.2018.06.079.

[56] International Organization for Standardization, ISO 12215-5: Small craft—Hull Construction, and scantlings—Part 5: Design Pressures for Monohulls, Design Stresses, Scantlings Determination, ISO, Geneva, 2019.

[57] Z. Han, J. Jang, J.-B.R.G. Souppez, H. Seo, D. Oh, Comparison of structural design and future trends in composite hulls: a regulatory review, Int. J. Nav. Archit. Ocean Eng. 15 (2023) 100558, https://doi.org/10.1016/j.ijnaoe.2023.100558.

[58] Z. Han, S. Jeong J. Noh, D. Oh, Comparative study of glass fiber content measurement methods for inspecting fabrication quality of composite ship structures, Appl. Sci. 10 (2020) 5130, https://doi.org/10.3390/app10155130.

[59] J. Jang, Z. Han, D. Oh, Light-weight optimum design of laminate structures of a GFRP fishing vessel, J. Ocean Eng. Technol. 33 (2019) 495–503, https://doi.org/10.26748/KSOE.2019.105.

[60] P. Wang, H. Lei, X. Zhu, H. Chen, D. Fang, Investigation on the mechanical properties of epoxy resin with void defects using digital image correlation and image-based finite element method, Polym. Test. 72 (2018) 223–231, https://doi.org/10.1016/j.polymertesting.2018.10.025.

[61] M. Mehdikhani, L. Gorbatikh, I. Verpoest, S.V. Lomov, Voids in fiber-reinforced polymer composites: a review on their formation, characteristics, and effects on mechanical performance, J. Compos. Mater. 53 (2018) 1579–1669, https://doi.org/10.1177/0021998318772152.

[62] Y. Li, B. Wang, L. Zhou, Study on the effect of delamination defects on the mechanical properties of CFRP composites, Eng. Fail. Anal. 153 (2023) 107576, https://doi.org/10.1016/j.engfailanal.2023.107576.

[63] D.S. Lobanov, S.V. Slovikov, E.M. Lunegova, Influence of internal technological defects on the mechanical properties of structural CFRP, Frat. Struct. Integr. 17 (65) (2023) 74–87, https://doi.org/10.3221/IGF-ESIS.65.06.

[64] S.-G. Lee, D. Oh, J.H. Woo, The effect of high glass fiber content and reinforcement combination on pulse-echo ultrasonic measurement of composite ship structures, J. Mar. Sci. Eng. 9 (2021) 379, https://doi.org/10.3390/jmse9040379.

[65] A.P. Mouritz, Ultrasonic and interlaminar properties of highly porous composites, J. Compos. Mater. 34 (2000) 218–239, https://doi.org/10.1177/002199830003400303.

[66] ASTM International, ASTM D3171-15: Test Methods for Constituent Content of Composite Materials, ASTM, West Conshohocken, 2015, https://doi.org/10.1520/D3171-15.

[67] P.V. Joseph, K. Joseph, S. Thomas, C.K.S. Pillai, V.S. Prasad, G. Groeninckx, M. Sarkissova, The thermal and crystallisation studies of short sisal fibre reinforced polypropylene composites, Compos. Part A Appl. Sci. Manuf. 34 (2003) 253–266, https://doi.org/10.1016/S1359-835X(02)00185-9.

[68] M. Fan, A. Naughton, Mechanisms of thermal decomposition of natural fibre composites, Compos. Part B Eng. 88 (2016) 1–10, https://doi.org/10.1016/j.compositesb.2015.10.038.

[69] ASTM International, ASTM D792-13: Standard Test Methods for Density and Specific Gravity (Relative Density) of Plastics by Displacement, ASTM, West Conshohocken, 2013, https://doi.org/10.1520/D0792-13.

[70] International Organization for Standardization, ISO 1172:2023 textile-glass-reinforced Plastics — Prepregs, Moulding Compounds and Laminates — Determination of the textile-glass and mineral-filler Content — Calcination Methods, ISO, Geneva, 2023.

[71] Z. Han, Y. Liu, X. Wu, D. Oh, J. Jang, Ultrasonic non-destructive inspection method for glass fibre reinforcement polymer (GFRP) hull plates considering design and construction characteristics, Proc. Inst. Mech. Eng. Part M J. Eng. Marit. Environ. 239 (2024) 156–165, https://doi.org/10.1177/14750902241245539.

[72] D. Klosterman, C. Browning, I. Hakim, K. Lach, Investigation of various techniques for controlled void formation in fiberglass/epoxy composites, J. Compos. Mater. 55 (2020) 489–506, https://doi.org/10.1177/0021998320952517.

[73] N. Abdelal, S.L. Donaldson, Comparison of methods for the characterization of voids in glass fiber composites, J. Compos. Mater. 52 (2017) 487–501, https://doi.org/10.1177/0021998317710083.

[74] I.A. Hakim, S.L. Donaldson, N.G. Meyendorf, C.E. Browning, Porosity effects on interlaminar fracture behavior in carbon fiber-reinforced polymer composites, Mater. Sci. Appl. 8 (2017) 170–187, https://doi.org/10.4236/msa.2017.82011.

[75] D. Oh, J. Jang, H.-H. Jee, Y. Kwon, S. Im, Z. Han, Effects of fabric combinations on the quality of glass fiber reinforced polymer hull structures, Int. J. Nav. Archit. Ocean Eng. 14 (2022) 100462, https://doi.org/10.1016/j.ijnaoe.2022.100462.

[76] H.-W. He, W. Huang, F. Gao, Comparison of four methods for determining fiber content of carbon fiber/epoxy composites, Int. J. Polym. Anal. Char. 21 (2016) 251–258, https://doi.org/10.1080/1023666X.2016.1139395.

[77] A. Beukers, E. Van Hinte, Lightness: the Inevitable Renaissance of Minimum Energy Structures, fourth ed., 010 Publishers, Rotterdam, 2005. https://books.google.co.kr/books?id=cBML479VZsEC&printsec=frontcover#v=onepage&q&f=false.

[78] J.-B.R.G. Souppez, P. Rodríguez Ruiz, M. Raihan, D. Oh, Experimental testing towards the regulatory inclusion of sustainable composite materials, J. Sailing Technol. 10 (2025) 171–190, https://doi.org/10.5957/jst/2025.10.1.171.

[79] J.E. Riccieri, L.H. De Carvalho, A. Vázquez, Interfacial properties and initial step of the water sorption in unidirectional unsaturated polyester/vegetable fiber composites, Polym. Compos. 20 (2004) 29–37, https://doi.org/10.1002/pc.10332.

[80] S.S. Shifa, M.H. Kanok, M.S. Haque, T. Sultan, K.F. Pritha, Mubasshira, et al., Influence of heat treatment and water absorption on mechanical properties of cotton-glass fiber reinforced epoxy hybrid composites: an eco-friendly approach for industrial materials, Hybrid Adv. 5 (2024) 100181, https://doi.org/10.1016/j.hybadv.2024.100181.

[81] S. Behera, R.K. Gautam, S. Mohan, A. Chattopadhyay, Hemp fiber surface modification: its effect on mechanical and tribological properties of hemp fiber reinforced epoxy composites, Polym. Compos. 42 (2021) 5223–5236, https://doi.org/10.1002/pc.26217.

[82] S. Sathish, K. Kumaresan, L. Prabhu, N. Vigneshkumar, Experimental investigation on volume fraction of mechanical and physical properties of flax and bamboo fibers reinforced hybrid epoxy composites, Polym. Polym. Compos. 25 (2017) 229–236, https://doi.org/10.1177/096739111702500309.

[83] F. Yao, Q. Wu, Y. Lei, W. Guo, Y. Xu, Thermal decomposition kinetics of natural fibers: activation energy with dynamic thermogravimetric analysis, Polym. Degrad. Stabil. 93 (2008) 90–98, https://doi.org/10.1016/j.polymdegradstab.2007.10.012.

[84] S. Oza, H. Ning, I. Ferguson, N. Lu, Effect of surface treatment on thermal stability of the hemp-PLA composites: correlation of activation energy with thermal degradation, Compos. Part B Eng. 67 (2014) 227–232, https://doi.org/10.1016/j.compositesb.2014.06.033.

[85] J. Chaishome, K.A. Brown, R. Brooks, M.J. Clifford, Thermal degradation of flax fibres as potential reinforcement in thermoplastic composites, Adv. Mater. Res. 894 (2014) 32–36. https://doi.org/10.4028/www.scientific.net/AMR.894.32.

[86] A.R. Horrocks, B.K. Kandola, Flammability and fire resistance of composites, in: A. C. Long (Ed.), Design and Manufacture of Textile Composites, Woodhead Publishing, Cambridge, 2005, pp. 330–363, https://doi.org/10.1533/9781845690823.330.

[87] Y.-C. Chiu, I.-C. Chou, W.-C. Tseng, C.-C.M. Ma, Preparation and thermal properties of diglycidylether sulfone epoxy, Polym. Degrad. Stabil. 93 (3) (2008) 668–676, https://doi.org/10.1016/j.polymdegradstab.2007.12.014.

[88] I. Chrysafi, N.M. Ainali, E. Xanthopoulou, A. Zamboulis, D.N. Bikiaris, Thermal degradation mechanism and decomposition kinetic studies of poly(ethylene succinate)/hemp fiber composites, J. Compos. Sci. 7 (2023) 216. https://www.mdpi.com/2504-477X/7/6/216.

[89] EcoTechilin, Response to Questions About Ecotechilin's FIBRIMAT F300 and FIBRIGHT H150 Products [Electronic Mail on the Internet], 2025, 2 July 2025.

[90] Easy Composites, 150g non-woven hemp fibre mat (480mm). https://www.easycomposites.co.uk/150g-non-woven-hemp-fibre-mat. (Accessed 21 July 2025).

[91] Easy Composites, 300g non-woven flax fibre mat (1000mm). https://www.easycomposites.co.uk/300g-non-woven-flax-fibre-mat. (Accessed 21 July 2025).

[92] Easy Composites, EL2 epoxy laminating resin. https://www.easycomposites.co.uk/el2-epoxy-laminating-resin. (Accessed 21 July 2025).

[93] Total Scale Solution Technology, Core tech HQ-DMF series HQ-DMF-3/4.5/14 2017. https://tstshop.co.kr/product/core-tech-%EC%BD%94%EC%95%84%ED%85%8C%ED%81%AC-hq-dmf-series-hq-dmf-3-45-14-%EB%94%94%EC%A7%80%ED%84%B8-%EC%A0%84%EA%B8%B0%EB%A1%9C-%ED%9A%8C%ED%99%94%EB%A1%9C-%EC%9A%A9%ED%95%B4%EB%A1%9C/451/. (Accessed 21 July 2021).

[94] L.L.C. Minitab, Minitab® Statistical Software, 2025, Version 19. https://www.minitab.com/en-us/products/minitab/.

[95] Y. Li, Q. Li, H. Ma, The voids formation mechanisms and their effects on the mechanical properties of flax fiber reinforced epoxy composites, Compos. Appl. Sci. Manuf. 72 (2015) 40–48, https://doi.org/10.1016/j.compositesa.2015.01.029.